

CDK2 and CDK4: Cell Cycle Functions Evolve Distinct, Catalysis-Competent Conformations, Offering Drug Targets

Wengang Zhang, Yonglan Liu, Hyunbum Jang, and Ruth Nussinov*



Cite This: *JACS Au* 2024, 4, 1911–1927



Read Online

ACCESS |

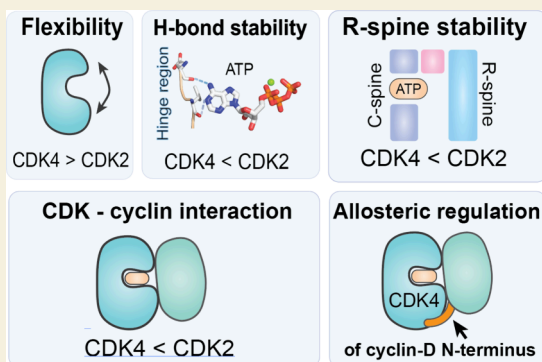
Metrics & More

Article Recommendations

Supporting Information

ABSTRACT: Cyclin-dependent kinases (CDKs), particularly CDK4 and CDK2, are crucial for cell cycle progression from the Gap 1 (G1) to the Synthesis (S) phase by phosphorylating targets such as the Retinoblastoma Protein (Rb). CDK4, paired with cyclin-D, operates in the long G1 phase, while CDK2 with cyclin-E, manages the brief G1-to-S transition, enabling DNA replication. Aberrant CDK signaling leads to uncontrolled cell proliferation, which is a hallmark of cancer. Exactly how they accomplish their catalytic phosphorylation actions with distinct efficiencies poses the fundamental, albeit overlooked question. Here we combined available experimental data and modeling of the active complexes to establish their conformational functional landscapes to explain how the two cyclin/CDK complexes differentially populate their catalytically competent states for cell cycle progression. Our premise is that CDK catalytic efficiencies could be more important for cell cycle progression than the cyclin-CDK biochemical binding specificity and that efficiency is likely the prime determinant of cell cycle progression. We observe that CDK4 is more dynamic than CDK2 in the ATP binding site, the regulatory spine, and the interaction with its cyclin partner. The N-terminus of cyclin-D acts as an allosteric regulator of the activation loop and the ATP-binding site in CDK4. Integrated with a suite of experimental data, we suggest that the CDK4 complex is less capable of remaining in the active catalytically competent conformation, and may have a lower catalytic efficiency than CDK2, befitting their cell cycle time scales, and point to critical residues and motifs that drive their differences. Our mechanistic landscape may apply broadly to kinases, and we propose two drug design strategies: (i) allosteric Inhibition by conformational stabilization for targeting allosteric CDK4 regulation by cyclin-D, and (ii) dynamic entropy-optimized targeting which leverages the dynamic, entropic aspects of CDK4 to optimize drug binding efficacy.

KEYWORDS: G1 cell cycle phase, G1/S transition, cyclin-dependent kinases (CDKs), allosteric drug discovery, cancer, ligand binding, CDK inhibitor, catalysis efficiency



1. INTRODUCTION

We ask: how exactly the catalytic phosphorylation of CDK4/cyclin-D was optimized by nature for the long G1 phase, whereas that of CDK2/cyclin-E, for the brief G1-to-S transition? That is, how do the two homologous complexes accomplish their catalytic actions with distinct efficiencies, tuned for their distinct functional roles in the cell cycle? The mammalian cell cycle is regulated by two protein families: the cyclins and the cyclin-dependent kinases (CDKs).¹ Proper progression through the cell cycle hinges on kinase activities of specific CDKs, which are primarily modulated by their interactions with cyclins. In the presence of their cyclin partners, CDKs function as serine/threonine kinases, regulating cell cycle progression by phosphorylating critical substrates such as the retinoblastoma protein (Rb).² CDK4/6 in conjunction with D-type cyclins (D1, D2, and D3) controls the early G1 phase, while the late G1 is controlled by CDK2 in conjunction with E-type cyclins (E1 and E2), resulting in a carefully orchestrated transition from the G1 phase to the S phase, where DNA

synthesis occurs.³ Cyclin-D/CDK4 partially phosphorylates the retinoblastoma (Rb) protein, releasing the E2F transcription factors. The freed E2F enables the transcription of S phase-related genes, predominantly cyclin-E. Cyclin-E then binds to CDK2, further phosphorylating Rb in a positive feedback loop, and fully activates E2F in the canonical model.⁴

Recent research has expanded the understanding of cell cycle control. Cells depend on sustained mitogen signaling and CDK4/6 activity to maintain CDK2 activity and Rb protein phosphorylation in a feed-forward loop, demonstrating that until mitosis, the decision to proliferate is reversible.⁵ The temporal integration of mitogenic signaling throughout the

Received: February 15, 2024

Revised: April 8, 2024

Accepted: May 6, 2024

Published: May 14, 2024



mother cell cycle can influence the daughter cell proliferation.⁶ These findings extend significantly the understanding of cell cycle commitment beyond the textbook model and suggest that the strength and duration of the mitogen signal have a profound influence not only on cell cycle commitment but also on the fate of the daughter cells.

Whereas the CDK levels are relatively constant throughout the cycle, the subcellular localization and concentrations of cyclins vary significantly, which facilitates selective activation of specific CDKs.⁷ The cellular levels of cyclins can impact the rate and extent of CDK activity and signal transduction. For instance, in many cancers, such as ovarian, breast, uterine, and gastroesophageal, overexpression of cyclin-E and cyclin-D leads to overactivity of CDK complexes, which ultimately leads to hyperproliferation of cells.⁸ While the differential expression and degradation of cyclins, their subcellular localization along with that of CDKs, mediated substrate specificity, and activation of different CDK complexes are crucial for cell cycle progression, they may not be the key essential element.⁹ Rather, it is the *catalytic activity level* of the CDKs that is more important for cell cycle progression.^{10,11} In regulating substrate phosphorylation, the cyclin acting in the G1 to S transition (especially cyclin-E) is influenced more by activity thresholds than by cyclin-substrate specificity.¹² Such findings are consistent with the understanding that CDK2 activity synchronizes cell cycle commitment and G1/S transition timing, and that high CDK2 activity is required to initiate the CDK2–Rb positive feedback loop, whereas CDK4/6 activity initiates E2F activity.¹³ This challenges the conventional understanding that the inherent biochemical specificity of cyclin/CDK complexes is the prime determinant of substrate phosphorylation. More importantly, these findings highlight the critical role of the level of CDK catalytic activity in regulating the cell cycle. However, the paramount question of exactly how evolution tuned and optimized the different cyclin/CDK complexes to modulate their corresponding phase of the cell cycle through their distinct catalytic activities was overlooked. However, resolving it is critical for understanding the principles underlying adapting catalytic activity to function, with vast biological as well as industrial implications.

Like other kinases, the catalytic activity of CDKs is influenced by both *intrinsic* and *extrinsic* factors.¹⁴ *Intrinsically*, key factors include the spatial arrangement of amino acid residues, the stability of the hydrophobic core, which includes the catalytic spine (C-spine), the regulatory spine (R-spine), and shell residues. The C-spine is composed of conserved hydrophobic residues that align with the adenine ring of ATP, playing a crucial role in ATP binding and orientation. The R-spine, also formed by hydrophobic residues, is parallel to the C-spine and is essential for stabilizing the active conformation of the kinase. Shell residues, bridging these spines, further contribute to the structural integrity of the kinase by interacting with both spines, supporting their proper alignment and stability.¹⁵ The flexibility of dynamic regions like the activation loop (A-loop) plays integral roles in substrate recognition, ATP binding, and phosphoryl transfer. Kinases exist in equilibrium between active and inactive conformations,¹⁶ and *extrinsic* binding of regulatory molecules or proteins can allosterically shift this equilibrium,¹⁷ enhancing, or dampening their activity.^{18,19} Among these, are p21 and p27 intrinsically disordered proteins that can inhibit or activate CDK2 and CDK4 depending on their phosphorylation state.²⁰ The catalytic activity of the kinase is a result of the integration

of various inputs at the allosteric sites, such as the binding of regulatory domains and substrates, and the effect of post-translational modifications, such as autophosphorylation.²¹

The crystal structures of the cyclin-E/CDK2 complex show the active conformation with cyclin-E contacting both the N- and C-lobe of CDK2 (Figure 1),²² whereas early structures of

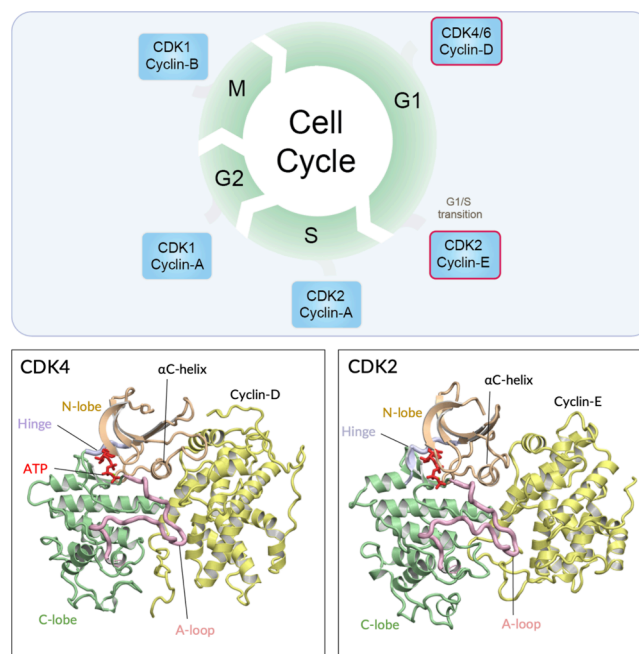


Figure 1. Cell cycle progression and cyclin-dependent kinase (CDK) complex structures. Upper panel illustrates the phases of the cell cycle, including G1, G1/S transition, and S, G2, and M phases, annotated with their corresponding cyclin and CDK complexes. The bottom panels display *in silico* modeled structures of the active cyclin-D/CDK4 and cyclin-E/CDK2 complexes, which are crucial for driving the cell cycle through the G1 and G1/S transition phases, respectively. ATP binding sites and structural features relevant to their kinase activity and regulatory mechanisms are labeled. Their sequence alignments are shown in Figure S1, which reveal high sequence similarity between CDK4 and CDK2, while low sequence similarity between cyclin-D and cyclin-E, yet their structural conformations in complex with their respective kinases are notably similar.

cyclin-D/CDK4 showed the inactive conformation with cyclin-D contacting only the N-lobe of CDK4,²³ leading to the expectation that CDK4 may require additional factors to reach the active state. Recently, the crystal structure of the active conformation of cyclin-D3/CDK4, in which cyclin-D3 contacts both the N- and C-lobes of CDK4, was resolved, showing significant differences from the early inactive conformations of cyclin-D/CDK4.^{23,24} One reason for the difference is that the cyclin N-terminus was not truncated prior to the crystallization, which was postulated to be the determining factor.²⁴ This suggests that even slight structural and conformational dynamical differences can lead to significant variations in how cyclin-D/CDK4 and cyclin-E/CDK2 activate, interact with, and modify their target substrates. Molecular dynamics (MD) simulations, with their ability to model protein motions and map allosterically coupled residue groups, have been especially useful in this context.²⁵

Here, we focus on the *active* conformations of CDK2 and CDK4 in complex with cyclins E and D, respectively, and seek to understand how the two cyclin/CDK complexes differ

entially populate their catalytically competent states. The role of enzyme dynamics is a long-standing question that traces back 40 years,²⁶ but still lacks clarity on the specific conformational changes that correlate to functional activities. Here, we find that upon activation, the cyclin-E/CDK2 complex has a greater ability to maintain the active features for catalysis. This includes CDK2 having a more compact nucleotide-binding site to stabilize ATP, a more stable R-spine, and more extensive contact with cyclin-E compared with the cyclin-D/CDK4 complex. Notably, full activation of cyclin-D/CDK4 requires additional stabilization of the A-loop by the N-terminus of cyclin-D, a requirement that is absent in the cyclin-E/CDK2 complex. This provides an additional obstacle to maximizing cyclin-D/CDK4's activity. Protein kinases that have a greater ability to maintain a stable hydrophobic core and stabilize ATP may offer a more efficient and conformationally favorable scenario.

2. MATERIALS AND METHODS

In this work, we implemented a comprehensive computational approach to contrast the dynamic behaviors and stability of cyclin-E/CDK2 and cyclin-D/CDK4 complexes, with a focus on ATP binding site stability, regulatory spine dynamics, protein–protein interaction profiles, and allosteric regulation mechanisms in the context of their roles in cell cycle regulation. Starting with MD simulations, we constructed the active conformations of these complexes. To quantify ATP-binding stability, we utilized potential of mean force (PMF) calculations to quantify the stability of ATP binding based on the key relevant active site interresidue distances, further backed by ATP-CDK interaction energies calculation, Principal component analysis (PCA), and pairwise residue distance-based calculation elucidated the major C- and N-lobe motions affecting the ATP-binding cleft. To quantify the overall stability of these kinases, a bioinformatics approach surveyed all available PDB structures of well-documented kinases, integrated with our MD simulations to delineate R-spine stability. Their stability and dynamic distinctions also reside in the CDK-cyclin binding interface. Binding free energy calculations allowed us to evaluate differences in the binding interactions between the two complexes, highlighting distinct interaction profiles. To build on that, alanine scanning calculations identified critical binding hotspots, indicating the structural determinants that are important for CDK-cyclin interaction specificity. This interaction specificity is further unraveled by chemical shift perturbation (CSP) analysis, which highlights the greater dependency of cyclin binding for the activation of CDK4, especially on the A-loop region. To further understand how CDK4 is allosterically activated, we mapped the influence of the cyclin-D N-terminus on the active site of CDK4 using dynamical network analysis via the Weighted Implementation of Suboptimal Paths (WISP) methodology. Ramachandran analysis of the DFG motif further supported these findings. Using these integrated approaches, we illustrate how these computational methods provide insights into the structural and dynamical determinants of kinase activity and regulation.

2.1. Modeling of CDK Complexes

We modeled the conformations of the complexes of CDK2 and CDK4 in their cyclin-bound states in the presence of ATP. The initial coordinates for the active cyclin-E/CDK2 and cyclin-D/CDK4 were taken from the crystal structures of the Protein Data Bank (PDB) with codes 1W98 and 7SJ3, respectively. Both structures are phosphorylated on the active site on the A-loop (pT172 on CDK4, and pT160 on CDK2). The inactive intermediate conformation of cyclin-D/CDK4 is modeled after the PDB code 2W9Z. All missing loops were added using the CHARMM package. We also simulated the active conformations of both CDK4 and CDK2 monomers as well as unphosphorylated A-loop from their crystal structures listed above for reference. ATP is docked into the active site in all these structures by

aligning an ATP-bound crystal structure (PDB code: 1FIN) to the PDB structures and removing the protein in 1FIN. The solvent was modeled using the TIP3P model with at least a 15 Å shell of water in each direction. The charge states of all titratable groups were set to reflect a neutral pH environment with acidic side chains represented in their negatively charged forms and basic side chains in their positively charged forms. We tabulate the simulation systems in Table S1. We used the TIP3P water model and added Na⁺ and Cl[−] to neutralize the solvated systems and maintain a physiological salt concentration of 150 mM.

2.2. MD Simulation Protocol

We utilized molecular dynamics (MD) simulations in accordance with the methodologies detailed in our previous publications.^{27–31} These simulations were executed in several steps. Initially, we undertook 10,000-step energy minimizations via the conjugate gradient minimization method to optimize the systems, which was important in removing undesirable atomic contacts. Subsequently, for every system, we conducted three 2 μs all-atom explicit-solvent MD simulations under the NPT ensemble (constant number of atoms, pressure, and temperature) and 3D periodic boundary conditions for each system. We used the NAMD 2.14 package³² for the production runs with the updated CHARMM³³ all-atom force field (version 36m).³⁴ We employed the Nosé–Hoover Langevin piston control to sustain the pressure at 1 atm and the Langevin thermostat to maintain the temperature constant at 310 K. The SHAKE algorithm was applied to constrain the covalent bonds involving hydrogen atoms, and a 2 fs time step was used in the simulations. The long-range electrostatic calculation was performed using the particle mesh Ewald (PME) method (grid spacing of 1.0 Å), and the short-range interactions were calculated using the switching functions for proximal van der Waals (vdW) interactions (twin-range cutoff at 12 and 14 Å). To ensure continuity in the potential energy function, nonbonding energy terms were gradually reduced to zero by implementing a smoothing factor starting at a distance of 12.0 Å.

2.3. Binding Free Energy Calculations

To quantitatively evaluate the affinity and specificity of the interactions between cyclin-D/CDK4 and cyclin-E/CDK2 complexes, we determined the binding free energies between cyclin-D and cyclin-E with CDK4 and CDK2, respectively, employing molecular mechanics energies combined with the generalized Born surface area (MM/GBSA) method. This calculation was performed using the CHARMM package.³³ The protocol adhered to established procedures from our previous works,^{27,35} ensuring consistency in our analysis.

The total binding free energy (ΔG_b) for the cyclin-CDK complexes is calculated as the sum of the gas-phase molecular mechanics energy (ΔE_{MM}), the solvation energy (ΔG_{sol}), and the entropy contribution ($-T\Delta S$), where T represents the temperature in Kelvin:

$$\langle \Delta G_b \rangle = \langle \Delta E_{MM} \rangle + \langle \Delta G_{sol} \rangle - T\Delta S$$

The ensemble average, indicated by angle brackets, aggregates these contributions over the last 1 μs configurations from the MD simulations. The gas-phase contribution, ΔE_{MM} , comprises internal energy (ΔH_{inter}), electrostatic interactions (ΔH_{elec}), and van der Waals interactions (ΔH_{vdW}):

$$\Delta E_{MM} = \Delta H_{inter} + \Delta H_{elec} + \Delta H_{vdW}$$

The solvation-free energy, ΔG_{sol} , integrates both the electrostatic and the nonpolar components. These are calculated using the generalized Born approximation with the generalized Born with a simple switching (GBSW) model within CHARMM:³⁶

$$\Delta G_{sol} = \Delta G_{sol}^{elec} + \Delta G_{sol}^{nonpolar}$$

Entropy contributions to the binding free energy are dissected into translational ($T\Delta S_{trans}$), rotational ($T\Delta S_{rot}$), and vibrational ($T\Delta S_{vib}$) components. These terms are estimated from the principal moments of inertia (for translational and rotational entropy) and calculated

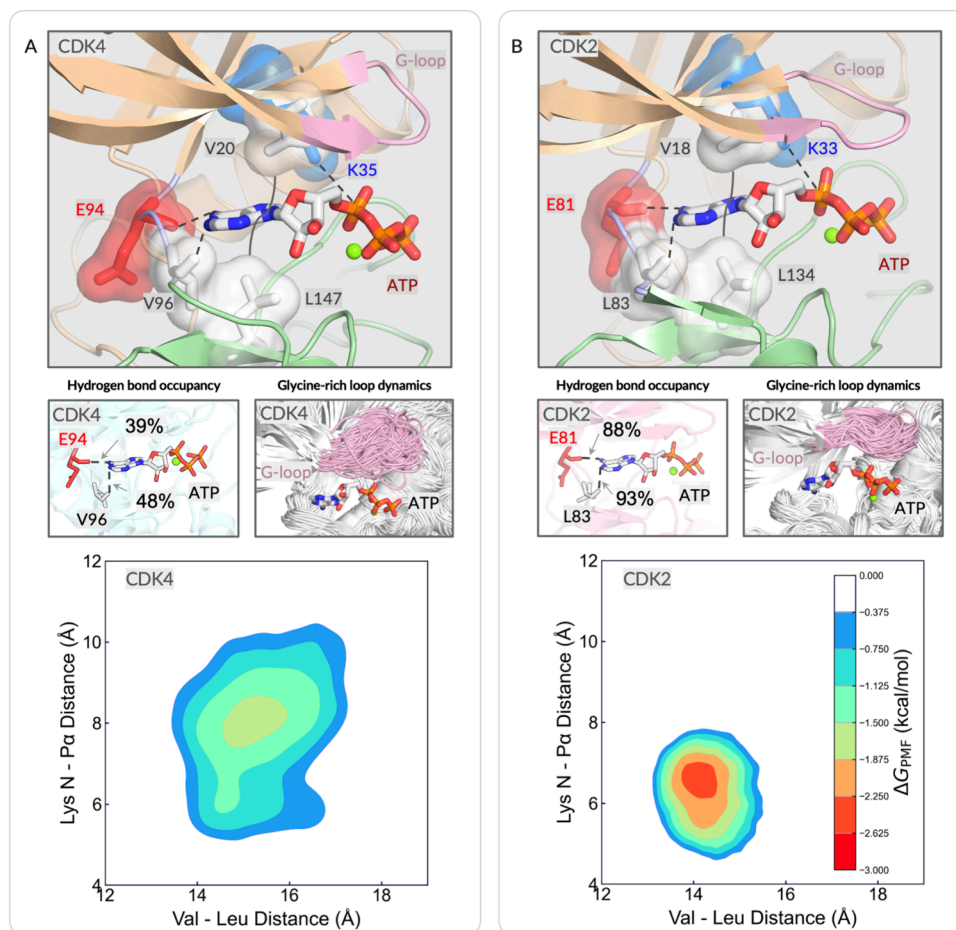


Figure 2. Differential ATP binding site dynamics between active CDK4 and CDK2 complexes suggest distinct catalytically competent states. (*Upper panel*) Structure of the active CDK4 (A) and CDK2 (B) complex in the active site. It shows some key structural determinants influencing ATP-binding dynamics: (i) Adenosine-CDK interaction: Adenosine ring of ATP forms hydrogen bonds with the hinge region of CDKs, which is important for ATP orientation and stability. (ii) Hydrophobic Val and Leu residues (V20 and L147 for CDK4; V18 and L134 for CDK2) on the top and bottom of adenosine ring in ATP; their proximity is linked to the ATP binding site's open or closed conformation. (iii) G-loop enclosure: (G-loop) caps the ATP binding site, providing another layer of stabilization on ATP. (iv) Phosphate stabilization: Lysine on $\beta 3$ (K35 for CDK4; K33 on CDK2) interacts with α/β -phosphate and Glu on the α C-helix, further securing ATP in its binding site. (*Middle panel*) Hydrogen bond stability: CDK2 exhibits a higher hydrogen bond occupancy with ATP, indicative of enhanced ATP stabilization compared to CDK4. (*Middle panel*) G-loop dynamics: the G-loop of CDK4 is more dynamic, suggesting a propensity to assume an open conformation. (*Lower panel*) Potential of mean force landscapes for two reaction coordinates—the distance between nitrogen on Lys (Lys-N) and α -phosphate (P α) of ATP, and the distance between the valine and leucine residues. Both distances are consistently greater in CDK4 indicating that CDK4 has a broader range of accessible conformations when it binds to ATP, suggesting greater conformational flexibility. In contrast, ATP-bound CDK2 shows a more constrained energy landscape. Specifically, the larger Val–Leu distance suggests that the ATP binding site tends to adopt a more open and flexible conformation, while the shorter Lys–N–P α distance suggests an enhanced ATP stabilization and potentially efficient phosphoryl transfer. The contour maps illustrate the energy profiles along these coordinates, showing that CDK4 has a shallow energetic barrier than does CDK2 for their ATP-bound states.

using the quasiharmonic approximation (for vibrational entropy) in the VIBRAN module of CHARMM:

$$T\Delta S = T(\Delta S_{\text{trans}} + \Delta S_{\text{rot}} + \Delta S_{\text{vb}})$$

Finally, the net change in binding free energy due to complex formation ΔG_b is determined by subtracting the sum of the binding free energies of the unbound proteins (CDK and cyclin) from that of the bound complex:

$$\Delta G_b = \Delta G_b^{\text{complex}} - (\Delta G_b^{\text{CDK}} + \Delta G_b^{\text{cyclin}})$$

2.4. Chemical Shift and Perturbation Calculations

To investigate the conformational changes of CDK2 and CDK4 upon binding to their respective cyclins, we calculate the chemical shifts and chemical shift perturbations (CSPs) using SHIFTX2,³⁷ analogous to nuclear magnetic resonance (NMR) spectroscopy. The chemical

shifts provide insight into the local electronic environments of specific nuclei, revealing conformational dynamics in solution. SHIFTX2 precisely calculates the chemical shift changes of the diamagnetic ^1H , ^{13}C , and ^{15}N atoms in protein residues. This accuracy is achieved using a substantial, high-quality database of training proteins, advanced machine learning techniques, and by considering a wide array of factors including $\chi 2$ and $\chi 3$ angles, solvent accessibility, hydrogen-bond geometry, pH, and temperature. CSPs were analyzed to identify the environmental changes around nuclei that are indicative of conformational transitions upon cyclin binding. The trajectories of active CDK2 and CDK4, both free and in complex with their respective cyclins (cyclin-D for CDK4 and cyclin-E for CDK2), were used for the chemical shift calculation. CSPs were subsequently determined by comparing the chemical shifts of the kinase in its free form with those in the cyclin-bound form. For each residue, we calculate the CSP ($\Delta\delta$) between the CDK monomer and its cyclin-

bound state using the formula: $\Delta\delta = \sqrt{\Delta\delta_H^2 + (0.154 \times \Delta\delta_N)^2}$, where $\Delta\delta_H$ and $\Delta\delta_N$ are the changes in the chemical shift of proton and nitrogen on the backbone of an amino acid, respectively, and 0.154 is the scaling factor.^{35,38}

2.5. Quantification and Statistical Analysis

Result analyses were carried out using the CHARMM, VMD,³⁹ MDAnalysis,⁴⁰ python, SHIFTX2,³⁷ PyMOL,⁴¹ WISP,⁴² FoldX,⁴³ and ProteinsPlus.⁴⁴ To ensure the reproducibility and statistical robustness of our simulations, a uniform protocol was adhered to across all systems. Each system was subjected to three independent simulations to account for the variability. The convergence of these simulations was monitored through several parameters: the potential energy, electrostatic energy, and root-mean-square deviation (RMSD) of the C α atoms of the proteins. These metrics were used to evaluate the stability and consistency of our trajectories. For a more reliable statistical analysis, we utilized data from the final 1 μ s of each simulation, ensuring that the system had reached equilibrium and that transient effects had diminished.

3. RESULTS

3.1. CDK2 in Complex with Cyclin-E Has a More Stable ATP Binding Site Than CDK4 in Complex with Cyclin-D

The interplay of protein dynamics and function has been a key theme in the literature.⁴⁵ The CDK and cyclin families are an excellent example of this, wherein the subtleties of molecular interactions and signaling strength dictate cellular functional outcomes.⁴⁶ The ability of kinases to stabilize ATP molecules is necessary but not sufficient for a kinase to catalyze the phosphoryl transfer reaction. To evaluate the ATP binding stability, we first examine several structural and dynamic differences in and near the ATP binding site for both cyclin-D/CDK4 and cyclin-E/CDK2 complexes, as follows: (i) the hydrogen bonds between the hinge region and the adenosine ring in the ATP, (ii) the dynamics of the glycine-rich loop (G-loop, GxGxxG motif) that serves as a lid to anchor the ATP, (iii) the distance between the hydrophobic residues at the top and bottom of the ATP (Val–Leu distance, V18 and L134 for CDK2; V20 and L147 for CDK4), and (iv) the distance between the α -phosphate (P α) of the ATP and the nitrogen atom on the side chain of the lysine (K35 for CDK4; K33 for CDK2) on the β strand (Lys–N–P α distance). An example is shown for CDK4 in complex with cyclin-D (Figure S2). Based on these criteria, we found that CDK4 has a less stable hydrogen bond interaction with ATP and large fluctuations in the G-loop (Figure 2A). In contrast, CDK2 has a more stable hydrogen bond interaction with ATP, showcased by its higher hydrogen bond occupancy and more stable G-loop conformation (Figure 2B). This observation aligns with the broader observations that kinase inhibitors often form stable hydrogen bonds with the hinge region to outcompete ATP.^{47,48} A dynamic ATP site can influence the substrate turnover rates. The dynamics involved in opening and closing the nucleotide lid can be a rate-limiting step in catalysis, a concept previously discussed in relation to other kinases.⁴⁹ Earlier studies emphasized the role of the G-loop in various kinases, acting as a crucial component to stabilize the ATP binding site.⁵⁰ CDK4's G-loop further confirms it, displaying tendencies to adopt open conformations, suggesting that potentially modulating ATP turnover rates in that open G-loop conformation is less likely to sufficiently stabilize the ATP for efficient catalysis. Root mean square fluctuations (RMSFs) of the G-loop show greater fluctuations in CDK4 compared to CDK2 (Figure S3). To quantitatively evaluate the stability of

ATP in the binding site, we calculated the potential of mean force (PMF) along two reaction coordinates, Val–Leu and Lys–N–P α distances. The Val and Leu residues, part of the C-spine, are selected due to their significance in the hydrophobic interactions that stabilize the kinase. These hydrophobic interactions play a crucial role in the orientation and stabilization of ATP within kinases.⁵⁰ Similarly, the Lys–N–P α distance was chosen due to the lysine residue's role in stabilizing the α - and β -phosphates of ATP.⁵¹ This interaction is pivotal for securing ATP in its binding site. This specific distance can be indicative of the strength of ATP binding, which influences the kinase's catalytic potential.

CDK4 has a broader and more varied free energy surface in the PMF (Figure 2A), whereas CDK2 has a more restricted free energy surface in the PMF (Figure 2B), indicating a more stable and possibly a more rigid ATP-binding conformation. Such stability could be reflective of CDK2's precise and efficient catalytic activity in the G1/S transition. Specifically, Val–Leu distance provides information about the spatial dynamics of the loose or compact ATP binding site,^{29,52} while Lys–N–P α distance informs about the ATP interaction and phosphoryl transfer potential. The PMF analysis revealed that these distances are consistently greater in CDK4 compared to CDK2, signifying a broader range of accessible conformations for CDK4 when bound to ATP. In contrast, the shorter Lys–N–P α distance in CDK2 points toward an enhanced ATP stabilization within its binding site, which could lead to a more accurate and efficient phosphate transfer. This characteristic of CDK2 could be critical for its role in the precise regulation of the G1/S transition. The larger Val–Leu distance observed in CDK4 implies that its ATP binding site tends to adopt a more open and flexible conformation. Overall, the ATP-bound state of CDK2 presents a more constrained energy landscape, suggesting a more precise and targeted mechanism of action for its ATP-bound state and its ability to maintain a potentially more catalytically competent state than that of CDK4. It is consistent with the stronger interaction energy between ATP and cyclin-E/CDK2 as compared to that of the CDK4 complex (Figure S4), which is also consistent with the in vitro experiments of the IC50 values of ATP with CDKs.⁵³

To further reaffirm the stability of the ATP binding site in these two complexes, we also evaluate the opening and closing of the active cleft by examining the distance between Gly (G15 for CDK4; G13 for CDK2) on the G-loop in the N-lobe and Gly (G160 for CDK4; G147 for CDK2) of the DFG motif in the C-lobe (Figure S5). It shows that the ATP binding site of CDK4 has a greater fluctuation in the active site than that of CDK2. This is further confirmed by principal component analysis (PCA) (Figure S6). CDK4 explores a greater range of conformational spaces than CDK2. The first principal component (PC1) derived from the PCA is the predominant motion observed in both CDK4 and CDK2 complexes, characterizing the opening and closing of the N- and C-lobes of these kinases. This motion reflects the dynamic changes of the active site, thereby influencing the binding and potentially the catalytic efficiency of the kinases.^{54,55} The DFG motif is a critical element in kinase and plays an essential role in ATP binding and catalysis. Its conformational state can significantly influence catalytic readiness. By examining the Ramachandran plot for this motif and comparing it to the catalytically primed structure of CDK2, we can assess how its flexibility or rigidity contributes to the overall functionality of the kinase. Our analysis reveals that the DFG motif of CDK4 occupies a larger

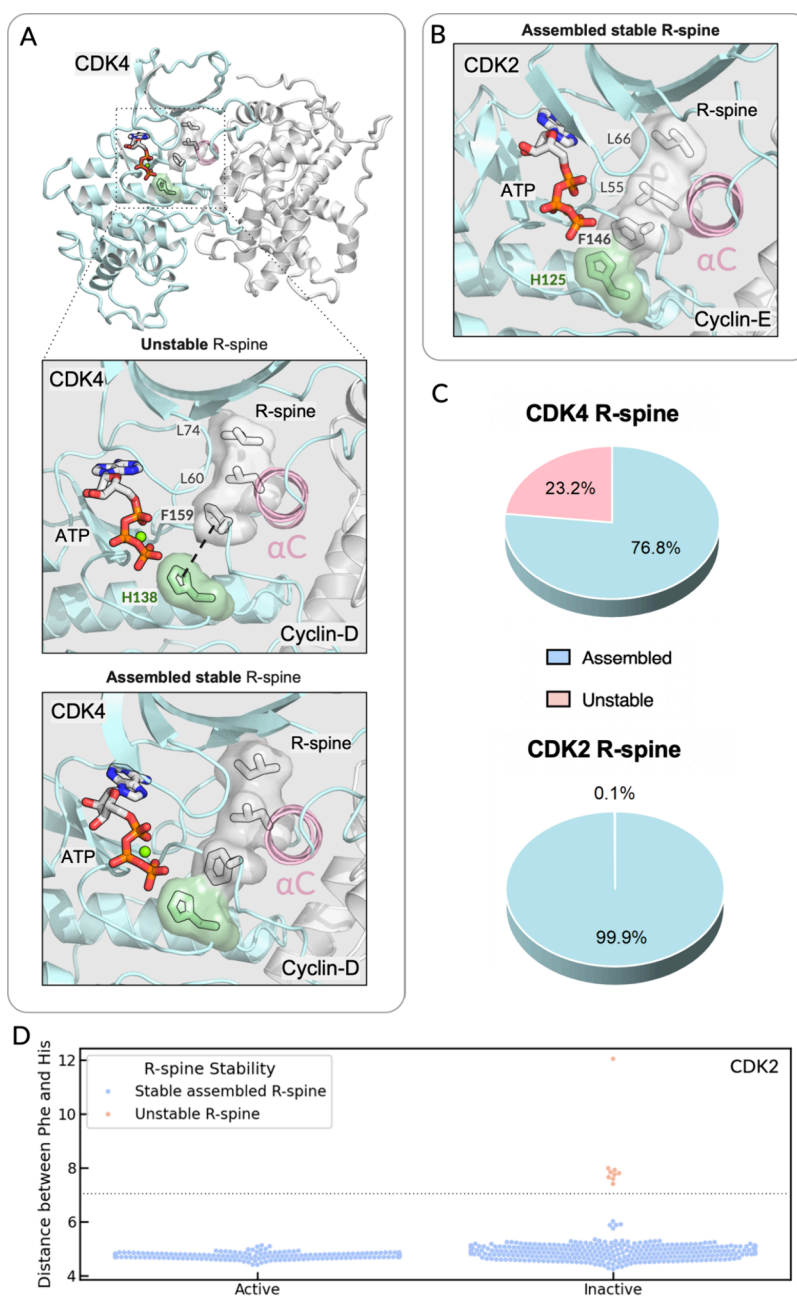


Figure 3. R-spine stability reveals CDK2's enhanced propensity for an active and assembled conformation. Stability of the R-spine is quantified by monitoring the distance between key residues, RS1, histidine (in the HRD-motif) and RS2, phenylalanine (in the DFG-motif), within the R-spine. (A) R-spine dynamics: for CDK4, the R-spine occasionally adopts unstable conformations deviating from the canonical, fully assembled state. To quantify the stability of the R-spine, we monitored the distance between the center of mass of the imidazole ring in histidine and the phenyl ring in phenylalanine residues within the spine. (B) CDK2 consistently, in contrast, maintains a more stable and fully assembled R-spine conformation throughout the simulations. (C) Likelihood for both CDK4 and CDK2 to adopt either a fully assembled or an unstable R-spine conformation. (D) Distances between Phe and His for all available PDB structures of CDK2 from the Protein Data Bank in Angstrom (\AA). The criteria for R-spine stability are based on the histidine-phenylalanine distance with the critical cutoff distances derived from an analysis of all publicly available PDB structures of CDK2 and CDK4, as well as numerous well-documented human kinases, including both inactive and active conformational states (Figure S11). Each data point represents a PDB structure. Through simulation data and PDB structure analysis, we identified a cutoff distance for R-spine stability: configurations are unstable above 7 \AA and stable below it.

phase space compared to CDK2 (Figure S7). This suggests that CDK4 has greater conformational flexibility within the DFG region. The DFG motif of CDK2 aligns relatively closely with the conformation seen in its catalytically primed structure, indicating a propensity to maintain a state conducive to efficient catalysis. This may be a key factor in the ability of the cyclin-E/CDK2 complex to effectively phosphorylate its

substrates during the G1/S transitions. Post-translational modifications such as phosphorylation at the active site the of A-loop (T172 for CDK4; T160 for CDK2) can also stabilize the complex, as shown in Figures S7 and S8. Taken together, our results show that CDK2 has a greater ability to stabilize ATP, which provides favorable conditions for cyclin-E/CDK2

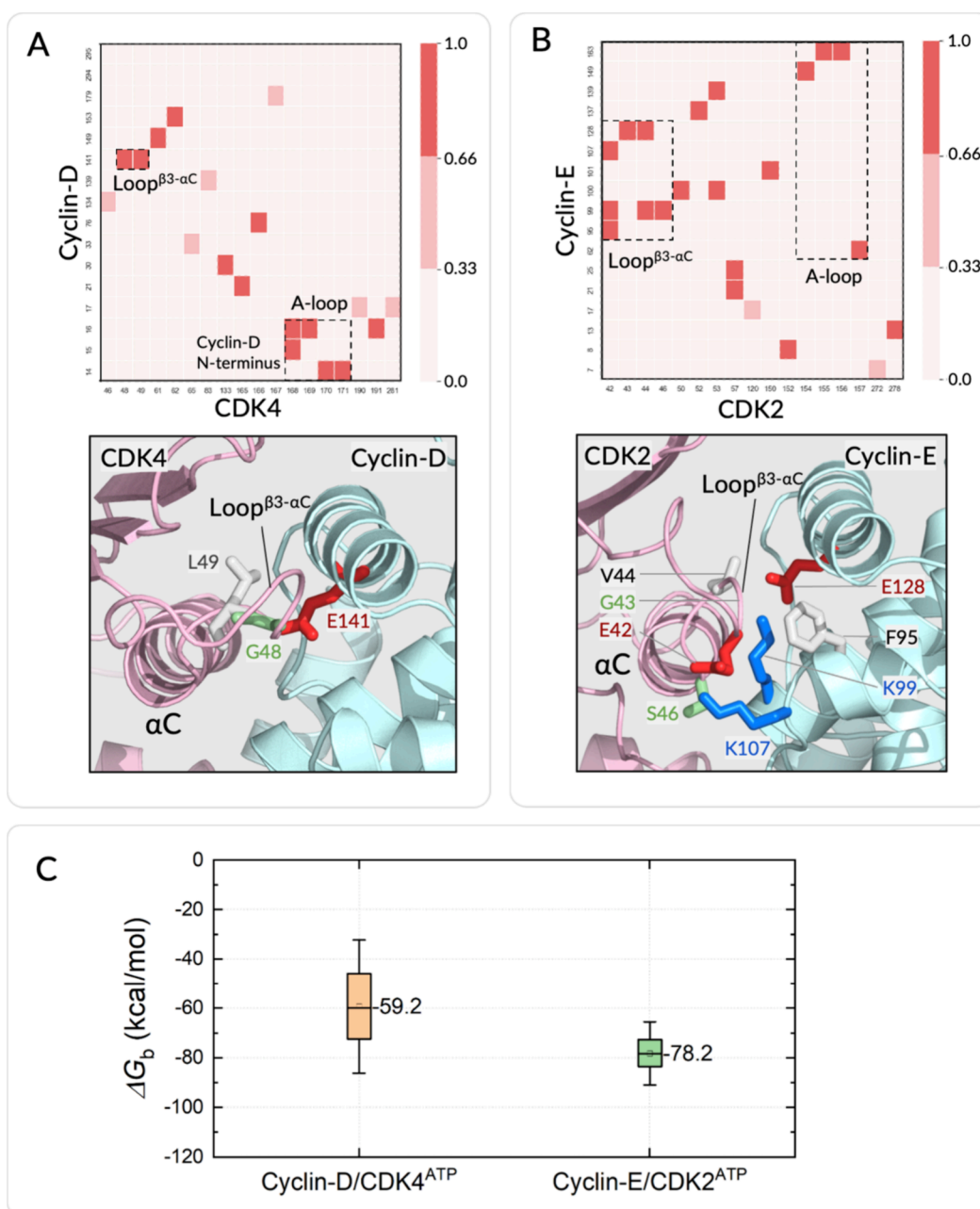


Figure 4. Differential interaction profiles between CDKs and their respective cyclins highlight CDK2's robust interface with cyclin-E. Contacting residue maps on the top row offer a dynamic representation of residue-wise interaction propensities between the CDKs and their partnering cyclins. It captures both transient and persistent contacts formed between the proteins. (A) CDK4 and cyclin-D interaction dynamics: CDK4 primarily forms persistent contacts with cyclin-D at residues L49 and G48 of the loop^{β3-αC}. Notably, the A-loop of CDK4 engages in extensive interactions with the N-terminus of cyclin-D, a distinct structural feature that underscores the specificity of their interaction. (B) CDK2 and cyclin-E interaction dynamics: CDK2 exhibits a more extensive interaction profile with cyclin-E, especially within the loop^{β3-αC} region. (C) CDK cyclin binding free energies ΔG_b for both CDK4 and CDK2 complexes. The box indicates 25–75% range, the whisker depicts the mean ± 1.5 SD, and the labels show the mean binding free energies. Cyclin-E/CDK2 complex has a lower binding free energy than that of cyclin-D/CDK4. We further identify loop^{β3-αC} and the A-loop in CDK2 as contributing significantly to the lower binding affinity of CDK2 complex, compared to that of the CDK4 complex using alanine scanning in Figure S12.

to maintain a catalytically preprimed state and thus potentially greater efficiency in catalysis than cyclin-D/CDK4.

3.2. Regulatory Spine (R-Spine) of CDK2 with Cyclin-E Is More Stable Than that of CDK4 with Cyclin-D

Kinase functionality hinges on multiple structural elements and their dynamics. Among them, the hydrophobic core typically consists of the catalytic-spine (C-spine, residues V20, A33, I146, L147, V148, L100, I203, M207 in CDK4; V18, A31, L87,

L133, L134, I135, I192, M196 in CDK2), shell residues (residues V72, F93, L91 in CDK4; V64, F80, L78 in CDK2), and regulatory spine (R-spine, residues RS1-H138, RS2-F159, RS3-L60, RS4-L74 in CDK4; RS1-H125, RS2-F146, RS3-L55, RS4-L66 in CDK2) providing the rigidity and stability needed for efficient transfer of the γ -phosphate (P_γ) of ATP.⁵⁶ The R-spine stands out. Previous studies have underscored its role in modulating kinase activity and shed light on how alterations in

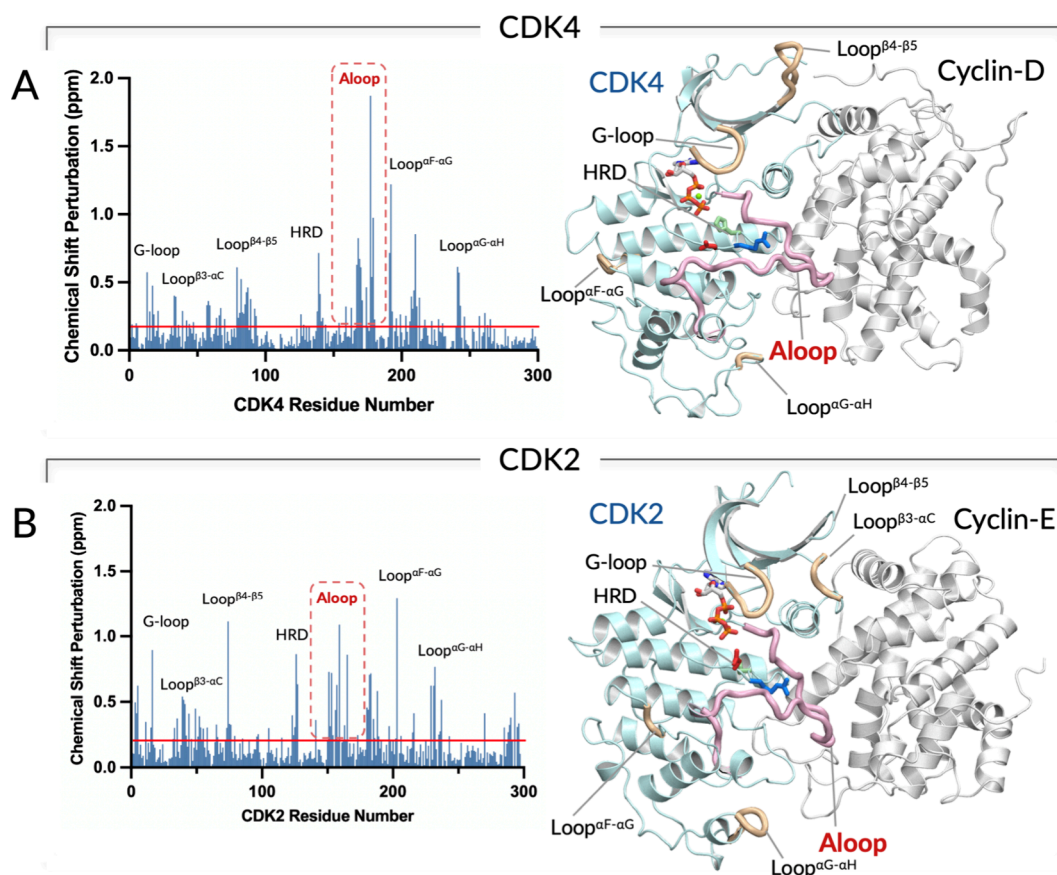


Figure 5. Differential roles of cyclin partners in A-loop stabilization highlight cyclin-D's importance in CDK4 activity regulation. We evaluate the chemical shift perturbations (CSPs) for active CDK complexes when their cyclin partners bind. (A) CDK4's chemical shift landscape: CSPs for active CDK4 are evaluated with key peaks annotated to map to specific structural features. The A-loop region of CDK4 showcases more residues, exhibiting pronounced chemical shifts. The magnitudes of these shifts are indicative of the role cyclin-D plays in stabilizing CDK4's activation loop. (B) In contrast to CDK2's chemical shift landscape, active CDK2 displays fewer and relatively diminished CSPs in its A-loop region. This suggests a comparatively subdued role for cyclin-E in stabilizing CDK2's A-loop, highlighting the unique regulatory dynamics between the two CDK-cyclin pairs. The red lines indicate the average CSP across all residues.

the R-spine can dictate conformational transitions between the active and inactive states.^{57,58} In our simulations, we observed distinct R-spine dynamics between CDK2 and CDK4 in their respective complexes. CDK4 sporadically displays unstable R-spine conformations, deviating from the fully assembled state (Figure 3A). In contrast, CDK2 maintains a more stable and fully assembled R-spine conformation compared with CDK4, suggesting a tendency toward a preorganized state for substrate binding and catalysis. Such dynamics modulate the kinase's affinity to substrates and influence its catalytic ability.⁵⁰ The R-spine of CDK4 stays fully assembled 76.8% of the time, while for CDK2, it is assembled almost the entire time (99.9%) (Figures 3B and S10B). This phenomenon is a common characteristic observed in many kinases. Based on the crystal structures of various kinases, it is evident that active kinases exhibit a preference for the well-assembled RS1-RS2 configuration of the R-spine, whereas inactive kinases prefer to adopt a disassembled RS1-RS2 (Figure S11). Furthermore, our analysis of other well-characterized kinases confirms a general trend: an active state correlates with a shorter RS1-RS2 distance, and an inactive state generally correlates with a longer RS1-RS2 distance (Figure S11). However, it is critical to recognize that some inactive kinases bound to small molecule inhibitors also exhibit a shorter RS1-RS2 distance. The pronounced stability of CDK2's R-spine can be one factor

driving its elevated catalytic activity,^{13,59} a finding that may be significant within the broader cell cycle regulatory mechanisms.

3.3. Stronger and More Robust Interactions between Cyclin-E and CDK2 Than that between Cyclin-D and CDK4

Cyclins are key regulators that promote the activation of CDKs. The interfaces between the kinases and cyclins, characterized by specific interaction profiles, provide insights into their functional modalities. Previous studies have highlighted the importance of these interfaces in kinase activity.⁶⁰ To explore the contrasting interaction profiles of cyclin-D/CDK4 and cyclin-E/CDK2, we examined the residue contact map, which represents the probability that two residues are in contact across all trajectories. We define two residues as contacting each other if the atoms of these residues, excluding hydrogen atoms, are within 3.5 Å of each other. We observed that the more extensive interaction profile on the CDK2 complex (Figure 4A) than the CDK4 complex (Figure 4B) appears to be potentially optimized for its efficient activation and phosphorylation, as evidenced by the more persistent contacting residues for the CDK2 complex (see more dark red squares in the figure). This is consistent with the stronger interaction between cyclin-E and CDK2 than cyclin-D and CDK4 (Figure 4C), detailed in Materials and Methods section 2.3. Comparing the interacting residues on the N-lobe of CDK2 and CDK4 with their respective cyclins, we observed

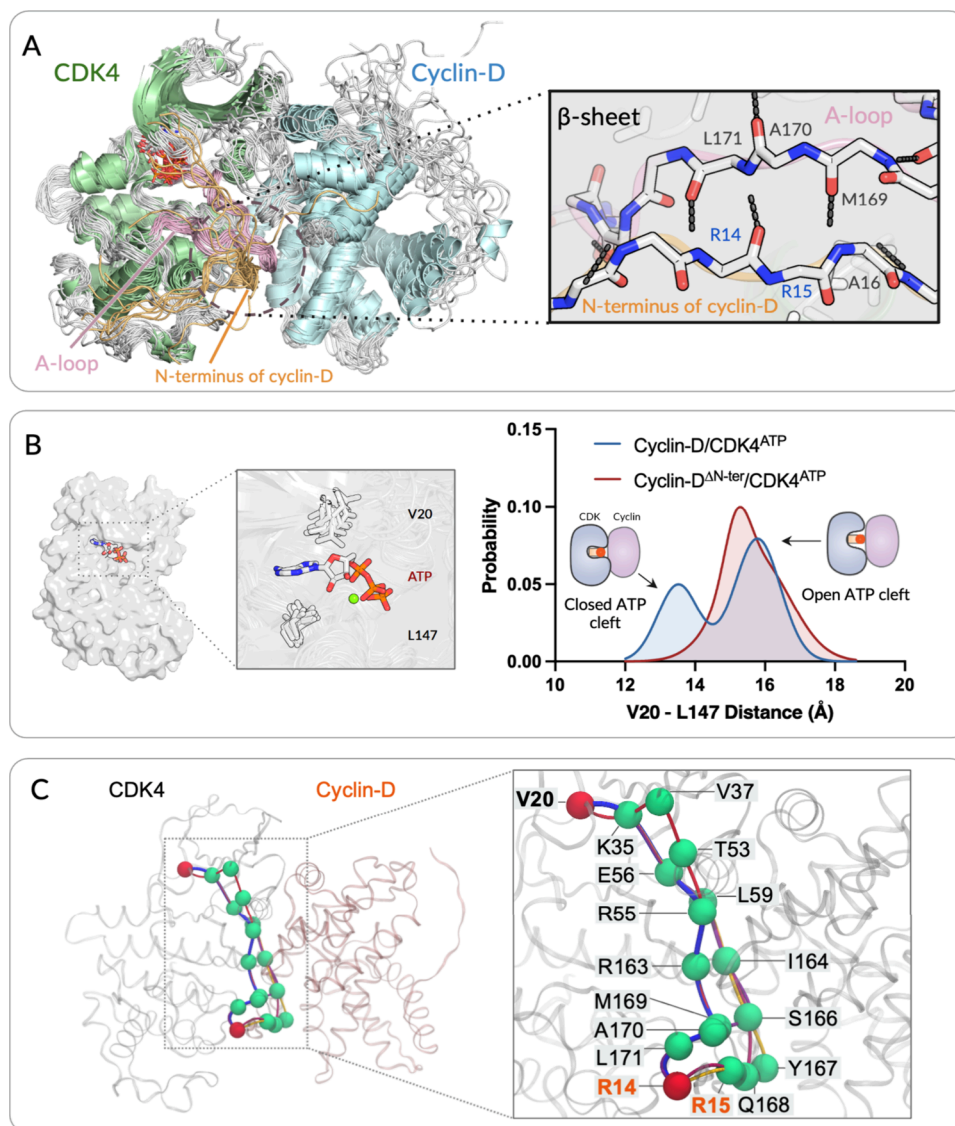


Figure 6. Cyclin-D's N-terminus acts as an allosteric regulator, governing the activation loop and ATP binding site conformation in CDK4. (A) N-terminus interactions with A-loop: the N-terminus of cyclin-D and the A-loop of CDK4 form a β -strand and hydrogen bonds with the A-loop, suggesting a structural interdependence critical for maintaining CDK4's active conformation. (B) Influence on the ATP binding site conformation: By evaluating the distance distribution between residues V20 and L147, we contrast the conformational behavior of the active cyclin-D/CDK4 complex with that of its counterpart, cyclin-D ^{Δ N-ter}/CDK4 (cyclin-D lacking the N-terminus). Notably, the absence of cyclin-D's N-terminus results in a pronounced shift in the ATP binding site's dynamics. This is evident from the diminished probability of the complex assuming a closed ATP binding site conformation, as indicated by the vanishing peak near the 13.5 Å mark in the red curve. (C) Allosteric pathways between the N-terminus of cyclin-D (R14 and R15) and V20 of CDK4. The source residues are either R14 or R15 in cyclin-D, and the sink residue is V20 in CDK4. Red beads represent the source and sink residues, while green beads denote the allosteric signal nodes. The blue lines represent the optimal, shortest allosteric pathway; lines of other colors indicate suboptimal allosteric pathways. The residue labels on the left-hand side identify the residues involved in the optimal allosteric pathway. This pathway shows that the source residue (R14) transmits the allosteric signal first through A-loop residues (L171, A170, M169, and R163) and then α C-helix residues (R55, and E56), followed by K35 on the β -strand, and finally reaches V20, a component of the C-spine. The residue labels with orange text indicate cyclin-D residues, while black text indicates CDK4 residues.

that only two residues on the loop ^{β 3- α C} of CDK4 (L49 and G48) form persistent contacts with cyclin-D, suggesting that the stable region of the interface is relatively small. In contrast, the loop ^{β 3- α C} of CDK2 forms more extensive interactions with cyclin-E. The A-loop of CDK4 in the C-lobe forms persistent contacts with the N-terminus of cyclin-D. To identify key residues critical for binding affinity and specificity, we conduct alanine scanning analysis using FoldX⁴³ to evaluate the binding energetics between CDK2/CDK4 and their cyclins (Figure S12). Our alanine scanning results align with our contacting residue maps, showing nearly identical contacting residues and

motifs for both complexes. Further, these contacting motifs exhibit more significant energy changes in the CDK2 complex than in the CDK4 complex, in both the number of contacting residues and the magnitude of energy changes, with these changes accounting for most of the interface energy variations in the alanine scanning, indicating their significance in contributing to the binding affinity between CDK and cyclin. This finding is consistent with the lower binding free energy of the CDK2 complex. The contacting residue maps in Figure 4 provide a dynamic view of the protein-protein interface, detailing the probability of residue contacts over time. This

dynamic perspective enhances the static analysis offered by alanine scanning, which evaluates the effect of alanine substitutions on binding affinity at a fixed point and identifies the binding hotspot. Integrating these methods allows us to capture both the dynamic and static elements of CDK-cyclin interactions, providing a more complete understanding of the conformational and energetic factors driving the specificity and stability of CDK-cyclin binding.

3.4. Activation Loop of CDK4 Is Stabilized by Its Cyclin Partner

The conformational changes of kinases upon binding to ligands can influence their catalytic activities. NMR spectroscopy, particularly chemical shift changes, can capture these structural dynamics in solution.⁶¹ Chemical shift perturbations (CSPs) can discern local environmental changes around specific nuclei, often associated with conformational transitions.⁶² CSP studies of kinases such as Abl, alpha-synuclein, and ERK, alongside segmental labeling in NMR techniques for proteins such as AKT and CDK2, have uncovered distinct mechanisms of allosteric inhibition and activation, offering profound insights that challenge and extend beyond traditional crystallography findings.^{19,63,64} Building on these studies, we used CSPs, detailed in Materials and Methods Section 2.4, to elucidate the differences in conformational changes of CDK2 and CDK4 as they bind to their respective cyclins. By plotting these CSPs along the protein sequence, we can identify the regions or specific residues that are most affected by cyclin binding. We first confirm that our results are consistent with general kinase NMR findings—an active kinase exhibits broadening of the amide resonances associated with catalytically important components such as the G-loop, DFG motif, and A-loop,⁵² which translate into peaks. Next, we compare the regulatory roles of cyclin-D for CDK4 and cyclin-E for CDK2 in the A-loop dynamics. Here our results show that the A-loop CSPs of CDK4 (Figure 5A) have more peaks of magnitude higher than those of CDK2 (Figure 5B), indicating more significant structural changes in the active conformation of CDK4 upon cyclin binding. This is consistent with the experimental study that highlighted the A-loop as part of a regulatory hub in kinase activity.⁶⁴ For CDK2, there is also a greater tendency toward A-loop extended conformation.⁶⁴ Cyclin-E induces smaller conformational changes on the A-loop of CDK2 than cyclin-D on the A-loop of CDK, suggesting that CDK2 may not require its cyclin partner to the same extent as CDK4 to remain in the active state and that cyclin-E/CDK2 has greater catalytic efficiency. The amplitude of these shifts not only reflects the important role of cyclin-D in A-loop stabilization but also suggests its critical role in the allosteric fine-tuning of CDK4 activity.

3.5. N-Terminus of Cyclin-D Acts As an Allosteric Regulator Necessary for Full activation of CDK4

The allosteric landscape of proteins is crucial for cellular processes.⁶⁵ It is particularly relevant in the context of kinases, where even subtle structural perturbations can elicit pronounced functional alterations.^{28,66} The aforementioned observations suggest that CDK2 adopts a more robust activation mechanism in the presence of the cyclin partner compared to CDK4. A recent study introduced a distinct cyclin-D/CDK4 complex (PDB code: 7SJ3) characterized by increased contacts between the two proteins, a β -sheet formed between the N-terminus of cyclin-D and the A-loop of CDK4.²⁴ This raises the question of whether CDK4

encounters greater challenges in achieving full activation. To test this hypothesis, we constructed alternative models of the cyclin-D/CDK4 complex with and without the N-terminus of cyclin-D based on the crystal structure and examined the structural and dynamic variations of the N-terminus of cyclin-D with the A-loop of CDK4. The N-terminus of cyclin-D not only contributes to the stabilization of a β -strand by establishing interactions with the A-loop of CDK4 but also implies a structural dependence that is critical for maintaining the active state of the kinase (Figure 6A). This is supported by the study in which the N-terminus of cyclin-D3 enhances the activation segment and plays a role in the transition to the active conformation of CDK4.²⁴ The distance between the conserved hydrophobic residues Val20 and Leu147 at the top and bottom of the adenosine ring of ATP, which are part of the C-spine residues, shows a divergence between full-length and truncated (without the N-terminus) cyclin-D in complex with active CDK4 (Figure 6B). The conformational probability distribution reveals that the absence of the N-terminus of cyclin-D significantly reduces the propensity of the complex to adopt a closed ATP-binding site conformation. To show how the N-terminus of cyclin-D *allosterically* modulates the conformations of the ATP-binding site of CDK4, we conducted dynamical network analysis and constructed the allosteric pathways using Weighted Implementation of Suboptimal Paths (WISP) methodology in Figure 6C.⁴² We uncover allosteric signaling pathways between the N-terminus of cyclin-D and Val20 on the C-spine of CDK4. As shown in Figure 2, Val20 is important for the conformation of the ATP binding site. The distance between Val20 (in the N-lobe) and Leu147 (in the C-lobe) indicates the opening and closing of the ATP binding cleft. The optimal allosteric pathway (blue lines in Figure 6C) shows a signal transmission mechanism. It demonstrates that the N-terminus of cyclin-D transmits the allosteric signal starting from the source residue (R14) first through the A-loop (L171, A170, M169, and R163), then the α C-helix (R55, and E56), followed by K35 on the β 3-strand, and finally reaches V20. The salt bridge formed between Lys35 and Glu56 upon activation is not only for the stabilization of ATP but also for transducing an allosteric signal from cyclin-D.

Having established the allosteric effect of the N-terminus of cyclin-D, we further show that the complex with the full-length cyclin-D more effectively maintains the active state akin to the catalytically primed kinase using Ramachandran analysis in Figure S13. We find that the Asp residue's positioning in the DFG motif of CDK4 complexes undergoes significant changes depending on whether cyclin-D is full-length or has its N-terminus removed. In complexes with full-length cyclin-D, the Asp residue aligns more closely with the catalytically primed conformation ($\varphi \approx 60^\circ$, $\psi \approx 80^\circ$), which shows the N-terminus' role in stabilizing the active state. However, removing the N-terminus shifts the Asp residue's positioning to $\varphi \approx -120^\circ$, $\psi \approx 90^\circ$, leading to increased conformational space and decreased stability, highlighting the N-terminus's importance for maintaining enzymatic activity.

Based on these findings, our comparative and comprehensive analysis validates the hypothesis that the N-terminus of cyclin-D not only forms a β -sheet with the A-loop of CDK4 stabilizing the kinase but also has an allosteric effect on the conformation of the ATP binding cleft as well as maintaining the active conformation of CDK4. Thus, the N-terminus of cyclin-D is another example of how allosteric regulation mechanisms could affect kinase functionality. This finding also

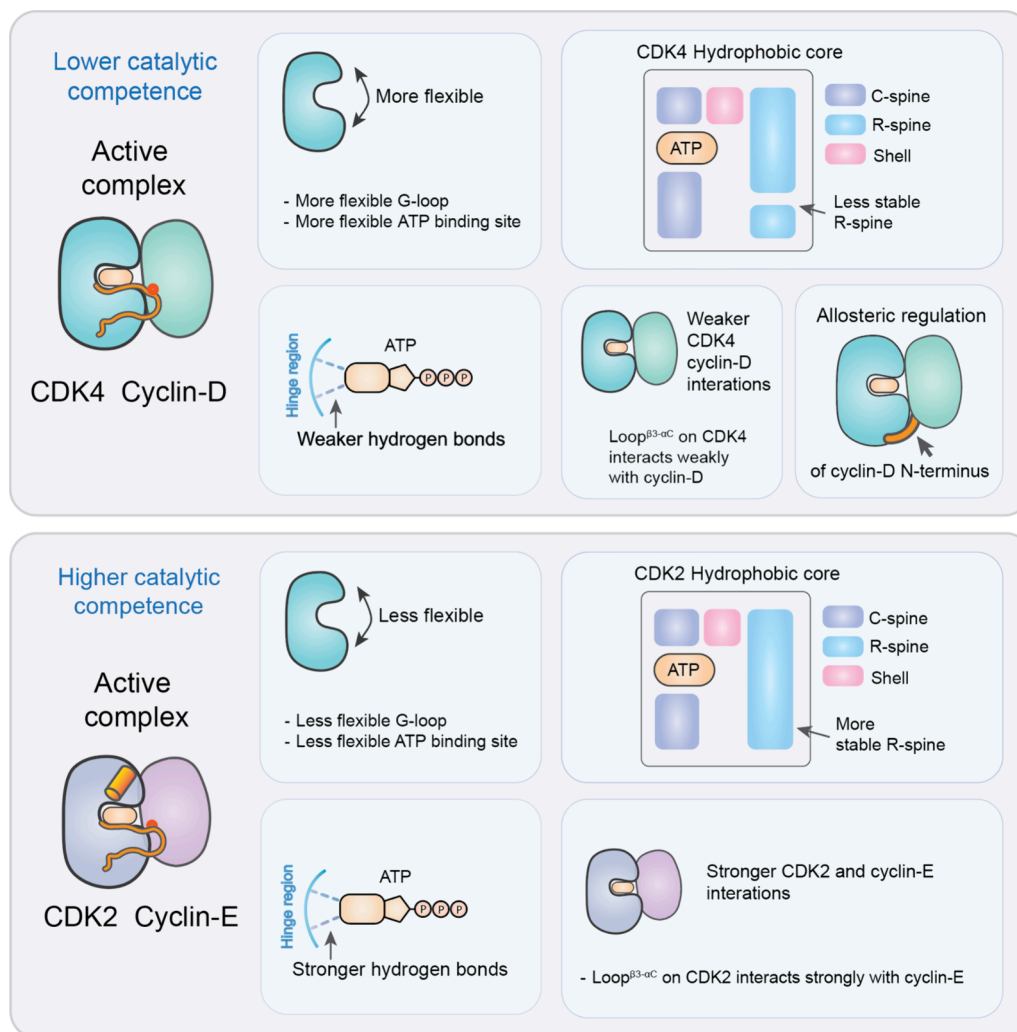


Figure 7. Differential conformational dynamics influence the stability of active cyclin-D/CDK4 and cyclin-E/CDK2 complexes and may affect their catalytically competent state. Key features of cyclin-D/CDK4/6: **ATP binding site dynamics:** CDK4's active state has a more expansive ATP binding site characterized by a highly flexible G-loop and varying distance between hydrophobic residues that sandwich ATP. **Suboptimal ATP binding:** the adenosine ring of ATP exhibits less stable hydrogen bond interactions with CDK4's hinge region, compared to the high occupancy of CDK2. **R-spine instability:** the hydrophobic core's R-spine in CDK4 shows reduced stability compared to its counterpart in CDK2. **Unique interactions with cyclin-D:** while CDK4's interactions with cyclin-D are limited (e.g., minimal contacts via loop^{β3-αC}), the contacts with cyclin-D's N-terminus are vital. This is emphasized by its role in A-loop stabilization through β -strand formation and its allosteric modulation of the ATP binding site's conformation.

accentuates the structural and functional importance of the A-loop and α C-helix in kinase activity regulation. In the CDK, they are important not only for substrate recognition, cyclin binding, and ATP positioning but also for transducing allosteric signaling.

4. DISCUSSION

The sequential activation and regulation of CDKs with their respective cyclins for cell cycle progression is well-established. But as to how specific cyclin-CDK pairs are differentiated in their cell cycle regulation, other than the oscillating concentration of their cyclins, and how they adapted to the distinct requirements of each cell cycle phase is less clear. In our previous work,³¹ we established the *speed and steps of activation* of these two distinct CDK complexes. Our findings demonstrated that cyclin-E/CDK2, with its faster activation time, is particularly suited for the shorter G1/S transition, whereas cyclin-D/CDK4, with a slower activation, aligns with

the longer G1 phase requirements. Here we ask *how active* cyclin-D/CDK4 in the G1 phase and cyclin-E/CDK2 in the G1/S transition phase have been *optimized* for their roles in substrate phosphorylation and signal transduction in cell cycle progression. We also ask what determinants regulate their activities.

We integrate our computational modeling with referenced experimental validations, such as mutagenesis, biochemical kinetics, X-ray crystal structures, and nucleotide affinity profiling studies, and propose five key structural and dynamic differences between the cyclin-D/CDK4 and cyclin-E/CDK2 complexes that may delineate the catalytic competence of these complexes (Figure 7). These include (i) the stability of the ATP-binding site, (ii) the ATP-CDK binding dynamics, (iii) the integrity of the hydrophobic core, especially the R-spine, (iv) the robustness of the CDK-cyclin interactions, and (v) the allosteric regulation mechanism of cyclin-D exerted on CDK4. Our findings, along with the referenced experimental validations, led us to propose a novel perspective on the role of

kinase structural stability, ATP stabilization capabilities, and more robust interactions with their regulatory proteins in maintaining their catalysis-primed states for effective substrate phosphorylation.

Our study highlights the dynamic nature of proteins, capturing CDK4's active site fluctuations on a nanosecond to microsecond time scale through MD simulations. This suggests that CDK4 has a more flexible active site than CDK2, potentially affecting its ATP stabilization and phosphoryl transfer efficiency. However, the dynamics involved in the catalytic cycle—spanning ATP binding to product release—extend beyond our simulation's scope, particularly noting that product release, often the rate-limiting step, and other key transitions occur on a longer millisecond time scale. Insights from adenylate kinase studies underline the significance of micro- to millisecond domain motions in enzyme functionality,⁶⁷ emphasizing that our findings may not fully capture these critical longer-time scale dynamics that influence catalytic efficiency. However, most important are the motions on the microsecond time scale between the open and closed states affecting the catalytic cycle that occurs on a much longer time scale.⁶⁷ Indeed, the active site of CDK4 shows a greater degree of fluctuations between open and closed conformations than that of CDK2 (Figure S4). Here, we propose that the excess dynamics of the ATP binding site and hydrophobic R-spine may negatively impact the kinase's catalytic competency due to its difficulty in stabilizing ATP effectively.

4.1. Integrating Computational Findings with Experimental Insights into ATP Stabilization in Kinase Activity

Among the factors influencing the kinetics of active CDK complexes, the ability of kinases to stabilize bound ATP molecules is one of the crucial determinants of their productive catalytic reaction. A stabilized ATP facilitates γ -phosphate transfer from ATP to the substrate protein, which requires precise coordination of the orientation and distance between the donor and acceptor groups. Like all enzymes, a kinase has single active and multiple inactive conformations. Higher flexibility of the ATP-bound conformation implies less time in the active, optimally coordinated conformation. We demonstrated that the cyclin-E/CDK2 complex has a greater ability to stabilize ATP than cyclin-D/CDK4, which may suggest that the CDK2 complex has a greater propensity to be in the catalytically competent state that may enable a faster phosphorylation rate.

We show four structural and dynamical restraints serving to fasten the ATP binding environment, providing all-around tethers: (i) the hydrogen bonds between the hinge region of a kinase and the adenosine ring of ATP. The conformational dynamics of these regions with ATP showcase the coordination required for optimal catalytic activities.⁶⁸ A quintessential feature is the adenosine ring of ATP, which engages in hydrogen bonding with the kinase's hinge region, which is critical for ensuring ATP orientation and stability.⁶⁸ Type-I kinase inhibitors are often optimized for robust hydrogen bonding between the hinge region and the inhibitors to outcompete ATP.⁴⁸ (ii) On the “top” and “bottom” of the ATP molecule, the conserved hydrophobic valine and leucine residues, as part of the C-spine, form hydrophobic network with the adenosine ring of ATP that stabilizes the entire kinase. The formation of the C-spine is vital for the kinase stability.⁶⁹ (iii) On the “lid” of the ATP molecule, the G-loop, which

partially collapses onto the ATP, creates a more buried, less solvent-exposed cavity, which can also contribute to kinase selectivity.⁷⁰ The G-loop of the active CDK4 complex exhibits significant dynamic states in contrast to the CDK2 complex. This observation is in line with the experimental results that CDK4 needs to have a G-loop sequence that mimics CDK6 for crystallization.²³ It is also consistent with the observation that the CDK4 β 1 strand and the following G-loop are not present in the p27-CDK4-cyclin-D1 trimer structure, indicating they are disordered.²⁰ The mechanism by which intrinsically disordered p27 inactivates CDK4 involves disruption of the CDK4 β 1 strand and G-loop,²⁰ pointing to the G-loop maintaining CDK4 active state. (iv) Lastly, the conserved lysine on the β 3 strand interacts with glutamic acid residue on the α C-helix, known to stabilize the kinase active conformation. It also binds to the α/β -phosphate of ATP and plays an important role in sensing ATP and enabling the transition of the kinase from the open to the intermediate state.^{51,71} The stability of ATP is necessary but not sufficient for the catalytically competent state.

Experimental mutagenesis studies also provide compelling support for our simulations, indicating that the stabilization of ATP plays a crucial role in influencing the ATPase rate. For instance, Coleman et al.⁷² demonstrated that mutations in CDK4, specifically CDK4-MUT6 (K35A on the β 3-strand) and CDK4-MUT13 (E94A, H95A in the hinge region), result in a decreased affinity for cyclin-D1 association, subsequently leading to reduced kinase activity. These mutations corroborate the insights that our simulation provides, with K35A mutations disrupting the critical Lys N–P α interaction and mutations in the hinge region affecting hydrogen bonds with ATP, thereby diminishing kinase function. Furthermore, Persky et al.⁷³ identified mutations in CDK4/6 that increase drug resistance, pointing to the significance of residues in the hinge region (CDK6-H100 or CDK4-H95) and the hydrophobic residues (CDK6-L152 or CDK4-L147) in the C-spine for ligand binding. Although this study primarily addresses inhibitor binding, it highlights the critical role that these residues play in ATP binding and suggests that alterations in these areas could similarly impact ATPase activity.

Biochemical kinetics, nucleotide affinity profiling, and single-cell experiments are also consistent with our findings and provide quantitative insights into the kinetic properties of cyclin-D1/CDK4 and cyclin-A/CDK2 complexes. The CDK4 complex shows a lower kinetic efficiency and a higher Michaelis constant for ATP compared to the CDK2 complex, which is compatible with our findings. Specifically, the Michaelis constant (K_m) for ATP in the cyclin-D1/CDK4 complex was determined to be 418 μ M, an unusually high value in comparison to cyclin-A/CDK2, which exhibited a K_m of 23 μ M.⁷⁴ This latter value aligns closely with those reported for most other regulatory protein kinases. In terms of turnover values, both cyclin-D1/CDK4 and cyclin-A/CDK2 complexes were estimated to have k_{cat} values of 3.4 and 3.9 min^{-1} , respectively.⁷⁴ A significant disparity in kinetic efficiency was observed, with cyclin-D1/CDK4 demonstrating over an order of magnitude lower efficiency (9.3 $\text{pM}^{-1} \text{min}^{-1}$) compared to cyclin-A/CDK2 (170 $\text{pM}^{-1} \text{min}^{-1}$).⁷⁴ This finding directly supports our proposition that the conformational dynamics of CDK4 are less stable than those of CDK2. Similarly, in an *in vitro* kinome-wide nucleotide affinity profiling study, the IC50 of ATP with CDK2 was identified as 66.9 μ M, utilizing CZK2 kinobeads.⁵³ While corresponding data for CDK4 is not

available, the closely related kinase, CDK6, showed an IC₅₀ value greater than 1000 μ M. These values, derived from noncycling cells, predominantly represent monomeric CDKs. This aligns with previous findings suggesting that apo-CDK4 naturally adopts a closed ATP binding conformation and requires cyclin-D binding to facilitate ATP binding site accessibility.³¹ Experiments using live-cell sensors monitoring CDK4/6 and CDK2 activities have shown that the rate of increase in CDK2 activity from the cumulative plot of activation is faster than that of CDK4/6 after mitogen stimulation, which suggests that the kinetics of CDK2 may be more efficient.^{11,13} Substrate phosphorylation can also be influenced by other factors. For instance, the phosphorylation of CDK1 on its targets and substrate specificity is influenced by the spatial arrangement and distances between multisite clusters, the nature of docking connections, the ratio of serine to threonine residues, etc.⁷⁵

4.2. Hydrophobic R-Spine Stability and Its Impact on Kinase Catalytic Efficiency

The hydrophobic R-spine, whose integrity is essential for kinase catalytic competency,^{54,56,68,76} is significantly more stable in active cyclin-E/CDK2 than cyclin-D/CDK4. Assembling of R-spine is typically initiated by some activation events such as cyclin binding in CDKs, such as the case for B-Raf dimerization and A-loop phosphorylation. When stable, the kinase often adopts an active conformation conducive to substrate binding and phosphoryl transfer. Instability can reduce the enzyme's efficiency. The significance of the spines in functionality is underscored by the oncogenic mutations, like the T334I mutation in chronic myeloid leukemia which reinforces the R-spine stability in the c-Abl kinase, leading to constitutive activation and reduced susceptibility to imatinib.⁷⁷ Similarly, B-Raf mutation L505F that enhances the hydrophobicity of R-spine has been shown to drive the assembly of the spine resulting in a strong, constitutively active kinase that does not need dimerization for activation.⁷⁸ Our findings highlight a key link between ATP binding stability and the integrity of the R-spine in kinases, particularly CDK complexes. The more stable ATP binding and robust hydrophobic R-spine in cyclin-E/CDK2 suggest a greater propensity for the kinase to remain in the active state and may lead to an enhanced catalytically competent state compared to cyclin-D/CDK4.

4.3. Allosteric Regulation and Implications for Drug Design

In terms of intermolecular interactions, we discover that the N-terminus of cyclin-D interaction with the A-loop allosterically shifts the ensemble toward the active state, modulating the ATP binding site conformation toward the closed conformation. Allostery is a common theme among kinases.^{57,79} However, this mechanism appears in contrast to cyclin-E, which does not require observable structural arrangement to engage with CDK2.²² CDK2 likely has a greater tendency to stay active and more efficient catalytically than CDK4, due to its less demanding need for β -strand formation with cyclin-E, reducing conformational constraints on its catalytic domain.

We can contextualize this allosteric regulation of the N-terminus of cyclin-D in CDK4 from two perspectives: (i) The terminal tails of a kinase or its modulators can play an important role in its activation and modulation. For example, the C-tail of AGC kinases, most notably PKA, extends into the ATP binding site and mediates hydrophobic interactions with the bound nucleotide, stabilizing it.^{15,80} Additionally, the C-

terminal helix of Rb and its exclusive interaction with cyclin-D/CDK4/6 supports its vital role in substrate recognition, and cell cycle progression, although structural details are unavailable.⁸¹ (ii) From the perspective of protein–protein interaction, the formation of β -strand between cyclin-D's N-terminus and CDK4's A-loop strengthens the interaction, which can lead to the shift of the kinase ensemble toward the active conformation, as in the case of mutant B-Raf (V600E and V600 K). B-Raf V600 K homodimers have stronger dimer interfaces than V600E. This results in more active dimers, increasing V600 K tumor aggressiveness.⁸²

We propose a novel drug design strategy, *allosteric inhibition by conformational stabilization*, to target CDK4 by exploiting the allosteric regulation exerted by cyclin-D.^{16,83} Stabilization (or destabilization) shifts the conformational ensemble and, as such, is an inherently allosteric event. Here, this strategy aims to inhibit CDK4 activation by stabilizing its inactive complex with cyclin-D, a concept based on the discovery that the N-terminus of cyclin-D allosterically modulates CDK4's ATP binding site. A crucial aspect of *allosteric inhibition by conformational stabilization* is the utilization of a previously unidentified drug-binding pocket within the inactive CDK4-cyclin-D complex (Figure S14), which could allow for highly selective inhibition. This pocket, revealed through our simulations, is accessible only when CDK4 is in an inactive state, characterized by the interaction of only CDK4's N-lobe with cyclin-D with conformational features like the α C-helix in an OUT conformation and a collapsed A-loop. The strategy focuses on disrupting the cyclin D's N-terminus interaction with CDK4's A-loop, aiming to block the full activation of the CDK4 by cyclin-D. Inspired by type III allosteric inhibitors targeting CDK2 and Src,^{58,84} *allosteric inhibition by conformational stabilization* seeks to extend this principle by targeting the C-lobe of CDK4 to inhibit its activation or cyclin-D binding. Our approach suggests a pathway to develop potent CDK4 inhibitors by leveraging the allosteric regulation mechanism exerted by cyclin-D.

In addition, we introduce another CDK4 drug design strategy named *dynamic entropy-optimized targeting*, specifically aimed at targeting the orthosteric binding pocket of the active CDK4 complex (α C-IN, A-loop extended). In traditional drug design, enhancing a lead compound's affinity to the target is typical but may not increase drug residence time due to transitional state compensation. Traditional designs often focus on enthalpic optimization based on static crystal structure and overlook target flexibility and conformational entropy, which are crucial in protein–ligand interactions.⁸⁵ Amaral et al. showed that entropically driven binding compounds exhibit slower association/dissociation rates, indicating that targeting protein dynamics enhances binding efficacy. Roscovitine, a CDK2 inhibitor, has a lower dissociation constant with the cyclin/CDK2 complex than monomeric CDK2,⁶⁴ likely due to the complex's reduced flexibility. This observation aligns with current drug design strategies, where optimization based on static protein–ligand complexes from crystal structures may favor compounds with a higher affinity for less flexible protein states. This insight informs our strategy: for CDK4, targeting its ligand-bound, flexible conformation could optimize drug binding efficacy. Specifically, by incorporating *entropic* considerations into ligand design and taking protein flexibility upon binding into account, we can create more effective inhibitors. For CDK4, this means designing ligands to take advantage of the drug-bound state flexibility. Ultimately, this

approach should balance enthalpic and entropic contributions, emphasizing entropic gains for CDK4 on drug binding.

In conclusion, the cell cycle is a crucial regulator of cell division, governing processes from physiologic proliferation to oncogenic transformations, and abnormal differentiation in neurodevelopmental disorders. Here, we aimed to understand how its cyclin/CDK complexes evolved to achieve their distinct, functionally optimized catalytic activities in the long G1 phase and short G1/S transition. We merged structural, conformational dynamics, and functional cell data to resolve how structure and conformational dynamics in *active* CDK2 and CDK4 complexes can breed their respective catalytically competent states and catalytic rates. Our findings provide a fundamental mechanistic understanding of cyclins/CDKs and their roles in cell cycle regulation, potentially transforming therapeutic interventions.

■ ASSOCIATED CONTENT

Supporting Information

The Supporting Information is available free of charge at <https://pubs.acs.org/doi/10.1021/jacsau.4c00138>.

Sequence alignment of CDK2 and CDK4; structure of the active CDK4 in complex with cyclin-D; root-mean-square fluctuation (RMSF) of the G-loop of CDK4 and CDK2; interaction energies between ATP and CDK complexes; distance between Gly (G15 for CDK4; G13 for CDK2) on the G-loop and Gly (G160 for CDK4; G147 for CDK2) of the DFG motif; principal component analysis (PCA) of CDK4 and CDK2 dynamics; Ramachandran plot for A-DFG (Ala-Asp-Phe-Gly) motif in CDK4 and CDK2; effects of phosphorylated active site (pT160 on CDK2 and pT172 on CDK4) on A-loop; Ramachandran plot for A-DFG motif in both phosphorylated and unphosphorylated A-loop in CDK4 and CDK2; distance between His and Phe (or RS1-RS2) residues; probability distribution of the distance between Phe and His residues in the R-spine of CDK4 and CDK2 complexes; Phe – His distances for many human kinase structures; alanine scanning for interface residues between CDK4 and cyclin-D, and CDK2 and cyclin-E; potential drug binding pocket between the C-lobe of CDK4 and cyclin-D; and summary of the simulations of CDK4 and CDK2 monomer and complexes (PDF)

■ AUTHOR INFORMATION

Corresponding Author

Ruth Nussinov – Computational Structural Biology Section, Frederick National Laboratory for Cancer Research, Frederick, Maryland 21702, United States; Department of Human Molecular Genetics and Biochemistry, Sackler School of Medicine, Tel Aviv University, Tel Aviv 69978, Israel; orcid.org/0000-0002-8115-6415; Email: NussinoR@mail.nih.gov

Authors

Wengang Zhang – Cancer Innovation Laboratory, National Cancer Institute, Frederick, Maryland 21702, United States; orcid.org/0000-0001-9653-6966

Yonglan Liu – Cancer Innovation Laboratory, National Cancer Institute, Frederick, Maryland 21702, United States

Hyunbum Jang – Computational Structural Biology Section, Frederick National Laboratory for Cancer Research, Frederick, Maryland 21702, United States; orcid.org/0000-0001-9402-4051

Complete contact information is available at:

<https://pubs.acs.org/10.1021/jacsau.4c00138>

Author Contributions

CRedit: **Wengang Zhang** conceptualization, data curation, formal analysis, investigation, methodology, resources, software, validation, visualization, writing-original draft, writing-review & editing; **Yonglan Liu** investigation, software, writing-review & editing; **Hyunbum Jang** conceptualization, investigation, methodology, project administration, resources, software, supervision, writing-review & editing; **Ruth Nussinov** conceptualization, funding acquisition, project administration, resources, supervision, writing-review & editing.

Notes

The authors declare no competing financial interest.

■ ACKNOWLEDGMENTS

This project was supported in whole or in part by federal funds from the National Cancer Institute, National Institutes of Health, under contract HHSN261201500003I. The contents of this publication do not necessarily reflect the views or policies of the Department of Health and Human Services, nor does mention of trade names, commercial products, or organizations imply endorsement by the U.S. government. This research was supported [in part] by the Intramural Research Program of the NIH, National Cancer Institute, Center for Cancer Research. All simulations had been performed using the high-performance computational facilities of the Biowulf cluster at the National Institutes of Health, Bethesda, MD (<https://hpc.nih.gov/>).

■ REFERENCES

- (1) Morgan, D. O. *The Cell Cycle: Principles of Control*; New Science Press, 2007.
- (2) Rubin, S. M. Deciphering the retinoblastoma protein phosphorylation code. *Trends Biochem. Sci.* **2013**, *38* (1), 12–19.
- (3) Malumbres, M.; Barbacid, M. Cell cycle, CDKs and cancer: a changing paradigm. *Nat. Rev. Cancer* **2009**, *9* (3), 153–166.
- (4) Rubin, S. M.; Sage, J.; Skotheim, J. M. Integrating Old and New Paradigms of G1/S Control. *Mol. Cell* **2020**, *80* (2), 183–192.
- (5) Cornwell, J. A.; Crncec, A.; Afifi, M. M.; Tang, K.; Amin, R.; Cappell, S. D. Loss of CDK4/6 activity in S/G2 phase leads to cell cycle reversal. *Nature* **2023**, *619* (7969), 363–370.
- (6) Min, M.; Rong, Y.; Tian, C.; Spencer, S. L. Temporal integration of mitogen history in mother cells controls proliferation of daughter cells. *Science* **2020**, *368* (6496), 1261–1265.
- (7) Arooz, T.; Yam, C. H.; Siu, W. Y.; Lau, A.; Li, K. K.; Poon, R. Y. On the concentrations of cyclins and cyclin-dependent kinases in extracts of cultured human cells. *Biochemistry-U.S.* **2000**, *39* (31), 9494–9501. Roskoski, R., Jr. Cyclin-dependent protein serine/threonine kinase inhibitors as anticancer drugs. *Pharmacol. Res.* **2019**, *139*, 471–488. Gookin, S.; Min, M.; Phadke, H.; Chung, M.; Moser, J.; Miller, I.; Carter, D.; Spencer, S. L. A map of protein dynamics during cell-cycle progression and cell-cycle exit. *PLoS Biol.* **2017**, *15* (9), No. e2003268.
- (8) Montalto, F. I.; De Amicis, F. Cyclin D1 in Cancer: A Molecular Connection for Cell Cycle Control, Adhesion and Invasion in Tumor and Stroma. *Cells* **2020**, *9* (12), No. 122648. Gallo, D.; Young, J. T. F.; Fourtounis, J.; Martino, G.; Alvarez-Quilon, A.; Bernier, C.; Duffy, N. M.; Papp, R.; Roulston, A.; Stocco, R. CCNE1 amplification is

- synthetic lethal with PKMYT1 kinase inhibition. *Nature* **2022**, *604* (7907), 749. Matthews, H. K.; Bertoli, C.; de Bruin, R. A. M. Cell cycle control in cancer. *Nat. Rev. Mol. Cell Bio* **2022**, *23* (1), 74–88.
- (9) Coudreuse, D.; Nurse, P. Driving the cell cycle with a minimal CDK control network. *Nature* **2010**, *468* (7327), 1074–1079.
- (10) Basu, S.; Greenwood, J.; Jones, A. W.; Nurse, P. Core control principles of the eukaryotic cell cycle. *Nature* **2022**, *607* (7918), 381–386. Schwarz, C.; Johnson, A.; Koivomagi, M.; Zatulovskiy, E.; Kravitz, C. J.; Doncic, A.; Skotheim, J. M. A Precise Cdk Activity Threshold Determines Passage through the Restriction Point. *Mol. Cell* **2018**, *69* (2), 253–264 e255.
- (11) Yang, H. W.; Cappell, S. D.; Jaimovich, A.; Liu, C.; Chung, M.; Daigh, L. H.; Pack, L. R.; Fan, Y.; Regot, S.; Covert, M.; Meyer, T. Stress-mediated exit to quiescence restricted by increasing persistence in CDK4/6 activation. *Elife* **2020**, *9*, No. e44571, DOI: 10.7554/eLife.44571.
- (12) Swaffer, M. P.; Jones, A. W.; Flynn, H. R.; Snijders, A. P.; Nurse, P. CDK Substrate Phosphorylation and Ordering the Cell Cycle. *Cell* **2016**, *167* (7), 1750–1761.e16.
- (13) Kim, S.; Leong, A.; Kim, M.; Yang, H. W. CDK4/6 initiates Rb inactivation and CDK2 activity coordinates cell-cycle commitment and G1/S transition. *Sci. Rep.* **2022**, *12* (1), No. 16810, DOI: 10.1038/s41598-022-20769-5.
- (14) Tong, M.; Pelton, J. G.; Gill, M. L.; Zhang, W.; Picart, F.; Seeliger, M. A. Survey of solution dynamics in Src kinase reveals allosteric cross talk between the ligand binding and regulatory sites. *Nat. Commun.* **2017**, *8* (1), 2160. Verkhivker, G. M. Making the invisible visible: Toward structural characterization of allosteric states, interaction networks, and allosteric regulatory mechanisms in protein kinases. *Curr. Opin Struct Biol.* **2021**, *71*, 71–78.
- (15) Taylor, S. S.; Wu, J.; Bruystens, J. G. H.; Del Rio, J. C.; Lu, T. W.; Kornev, A. P.; Ten Eyck, L. F. From structure to the dynamic regulation of a molecular switch: A journey over 3 decades. *J. Biol. Chem.* **2021**, *296*, No. 100746.
- (16) Nussinov, R.; Jang, H.; Gursoy, A.; Keskin, O.; Gaponenko, V. Inhibition of Nonfunctional Ras. *Cell Chem. Biol.* **2021**, *28* (2), 121–133.
- (17) Nussinov, R.; Liu, Y.; Zhang, W.; Jang, H. Protein conformational ensembles in function: roles and mechanisms. *RSC Chemical Biology* **2023**, *4*, 850.
- (18) Levina, A.; Fleming, K. D.; Burke, J. E.; Leonard, T. A. Activation of the essential kinase PDK1 by phosphoinositide-driven trans-autophosphorylation. *Nat. Commun.* **2022**, *13* (1), 1874.
- (19) Skora, L.; Mestan, J.; Fabbro, D.; Jahnke, W.; Grzesiek, S. NMR reveals the allosteric opening and closing of Abelson tyrosine kinase by ATP-site and myristoyl pocket inhibitors. *Proc. Natl. Acad. Sci. U. S. A.* **2013**, *110* (47), E4437–4445.
- (20) Guiley, K. Z.; Stevenson, J. W.; Lou, K.; Barkovich, K. J.; Kumarasamy, V.; Wijeratne, T. U.; Bunch, K. L.; Tripathi, S.; Knudsen, E. S.; Witkiewicz, A. K.; et al. p27 allosterically activates cyclin-dependent kinase 4 and antagonizes palbociclib inhibition. *Science* **2019**, *366* (6471), No. eaaw2106, DOI: 10.1126/science.aaw2106.
- (21) Mingione, V. R.; Paung, Y.; Outhwaite, I. R.; Seeliger, M. A. Allosteric regulation and inhibition of protein kinases. *Biochem. Soc. Trans.* **2023**, *51* (1), 373–385.
- (22) Honda, R.; Lowe, E. D.; Dubinina, E.; Skamnaki, V.; Cook, A.; Brown, N. R.; Johnson, L. N. The structure of cyclin E1/CDK2: implications for CDK2 activation and CDK2-independent roles. *EMBO J.* **2005**, *24* (3), 452–463.
- (23) Takaki, T.; Echalié, A.; Brown, N. R.; Hunt, T.; Endicott, J. A.; Noble, M. E. M. The structure of CDK4/cyclin D3 has implications for models of CDK activation. *P Natl. Acad. Sci. USA* **2009**, *106* (11), 4171–4176. Day, P. J.; Cleasby, A.; Tickle, I. J.; O'Reilly, M.; Coyle, J. E.; Holding, F. P.; McMenamin, R. L.; Yon, J.; Chopra, R.; Lengauer, C.; Jhoti, H. Crystal structure of human CDK4 in complex with a D-type cyclin. *P Natl. Acad. Sci. USA* **2009**, *106* (11), 4166–4170.
- (24) Gharbi, S. I.; Pelletier, L. A.; Espada, A.; Gutierrez, J.; Sanfeliciano, S. M. G.; Rauch, C. T.; Ganado, M. P.; Baquero, C.; Zapatero, E.; Zhang, A.; et al. Crystal structure of active CDK4-cyclin D and mechanistic basis for abemaciclib efficacy. *NPJ. Breast Cancer* **2022**, *8* (1), 126.
- (25) Ahuja, L. G.; Aoto, P. C.; Kornev, A. P.; Veglia, G.; Taylor, S. S. Dynamic allostery-based molecular workings of kinase:peptide complexes. *Proc. Natl. Acad. Sci. U. S. A.* **2019**, *116* (30), 15052–15061.
- (26) Careri, G.; Fasella, P.; Gratton, E. Enzyme dynamics: the statistical physics approach. *Annu. Rev. Biophys. Bioeng.* **1979**, *8*, 69–97.
- (27) Liu, Y. L.; Jang, H.; Zhang, M. Z.; Tsai, C. J.; Maloney, R.; Nussinov, R. The structural basis of BCR-ABL recruitment of GRB2 in chronic myelogenous leukemia. *Biophys. J.* **2022**, *121* (12), 2251–2265.
- (28) Liu, Y.; Zhang, M.; Tsai, C. J.; Jang, H.; Nussinov, R. Allosteric regulation of autoinhibition and activation of c-Abl. *Comput. Struct Biotechnol J.* **2022**, *20*, 4257–4270.
- (29) Zhang, M. Z.; Maloney, R.; Jang, H.; Nussinov, R. The mechanism of Raf activation through dimerization. *Chem. Sci.* **2021**, *12* (47), 15609–15619.
- (30) Jang, H.; Smith, I. N.; Eng, C.; Nussinov, R. The mechanism of full activation of tumor suppressor PTEN at the phosphoinositide-enriched membrane. *iScience* **2021**, *24* (5), No. 102438. Jang, H.; Zhang, M. Z.; Nussinov, R. The quaternary assembly of KRas4B with Raf-1 at the membrane. *Comput. Struct Biotech* **2020**, *18*, 737–748.
- (31) Zhang, W.; Liu, Y.; Jang, H.; Nussinov, R. Slower CDK4 and faster CDK2 activation in the cell cycle. *Structure* **2024**, DOI: 10.1016/j.str.2024.04.012.
- (32) Phillips, J. C.; Braun, R.; Wang, W.; Gumbart, J.; Tajkhorshid, E.; Villa, E.; Chipot, C.; Skeel, R. D.; Kale, L.; Schulten, K. Scalable molecular dynamics with NAMD. *J. Comput. Chem.* **2005**, *26* (16), 1781–1802.
- (33) Brooks, B. R.; Brooks, C. L.; Mackerell, A. D.; Nilsson, L.; Petrella, R. J.; Roux, B.; Won, Y.; Archontis, G.; Bartels, C.; Boresch, S.; et al. CHARMM: The Biomolecular Simulation Program. *J. Comput. Chem.* **2009**, *30* (10), 1545–1614.
- (34) Huang, J.; Rauscher, S.; Nawrocki, G.; Ran, T.; Feig, M.; de Groot, B. L.; Grubmüller, H.; MacKerell, A. D. CHARMM36m: an improved force field for folded and intrinsically disordered proteins. *Nat. Methods* **2017**, *14* (1), 71–73. Klauda, J. B.; Venable, R. M.; Freites, J. A.; O'Connor, J. W.; Tobias, D. J.; Mondragon-Ramirez, C.; Vorobyov, I.; MacKerell, A. D., Jr.; Pastor, R. W. Update of the CHARMM all-atom additive force field for lipids: validation on six lipid types. *J. Phys. Chem. B* **2010**, *114* (23), 7830–7843.
- (35) Jang, H.; Banerjee, A.; Marcus, K.; Makowski, L.; Mattos, C.; Gaponenko, V.; Nussinov, R. The Structural Basis of the Farnesylated and Methylated KRas4B Interaction with Calmodulin. *Structure* **2019**, *27* (11), 1647.
- (36) Im, W.; Lee, M. S.; Brooks, C. L.; 3rd. Generalized born model with a simple smoothing function. *J. Comput. Chem.* **2003**, *24* (14), 1691–1702.
- (37) Han, B.; Liu, Y.; Ginzinger, S. W.; Wishart, D. S. SHIFTX2: significantly improved protein chemical shift prediction. *J. Biomol NMR* **2011**, *50* (1), 43–57.
- (38) Ruidiaz, S. F.; Dreier, J. E.; Hartmann-Petersen, R.; Kragelund, B. B. The disordered PCI-binding human proteins CSNAP and DSS1 have diverged in structure and function. *Protein Sci.* **2021**, *30* (10), 2069–2082.
- (39) Humphrey, W.; Dalke, A.; Schulten, K. VMD: Visual molecular dynamics. *J. Mol. Graph Model* **1996**, *14* (1), 33–38.
- (40) Michaud-Agrawal, N.; Denning, E. J.; Woolf, T. B.; Beckstein, O. MDAnalysis: a toolkit for the analysis of molecular dynamics simulations. *J. Comput. Chem.* **2011**, *32* (10), 2319–2327.
- (41) DeLano, W. L. *The PyMOL Molecular Graphics System*. Delano Scientific, 2002.
- (42) Van Wart, A. T.; Durrant, J.; Votapka, L.; Amaro, R. E. Weighted Implementation of Suboptimal Paths (WISP): An Optimized Algorithm and Tool for Dynamical Network Analysis. *J. Chem. Theory Comput* **2014**, *10* (2), 511–517.

- (43) Schymkowitz, J.; Borg, J.; Stricher, F.; Nys, R.; Rousseau, F.; Serrano, L. The FoldX web server: an online force field. *Nucleic Acids Res.* **2005**, *33*, W382–388. (Web Server issue)
- (44) Schoning-Stierand, K.; Diedrich, K.; Ehr, C.; Flachsenberg, F.; Graef, J.; Sieg, J.; Penner, P.; Poppinga, M.; Ungeth, A.; Rarey, M. ProteinsPlus: a comprehensive collection of web-based molecular modeling tools. *Nucleic Acids Res.* **2022**, *50* (W1), W611–W615.
- (45) Karplus, M.; Kuriyan, J. Molecular dynamics and protein function. *Proc. Natl. Acad. Sci. U. S. A.* **2005**, *102* (19), 6679–6685.
- (46) Nussinov, R.; Tsai, C. J.; Jang, H. Allostery, and how to define and measure signal transduction. *Biophys. Chem.* **2022**, *283*, No. 106766.
- (47) Derewenda, Z. S.; Hawro, I.; Derewenda, U. C—H ··· O hydrogen bonds in kinase-inhibitor interfaces. *IUBMB Life* **2020**, *72* (6), 1233–1242.
- (48) Roskoski, R., Jr. Properties of FDA-approved small molecule protein kinase inhibitors: A 2023 update. *Pharmacol. Res.* **2023**, *187*, No. 106552.
- (49) Hanson, J. A.; Duderstadt, K.; Watkins, L. P.; Bhattacharyya, S.; Brokaw, J.; Chu, J. W.; Yang, H. Illuminating the mechanistic roles of enzyme conformational dynamics. *Proc. Natl. Acad. Sci. U. S. A.* **2007**, *104* (46), 18055–18060.
- (50) Kornev, A. P.; Taylor, S. S. Dynamics-Driven Allostery in Protein Kinases. *Trends Biochem. Sci.* **2015**, *40* (11), 628–647.
- (51) Kornev, A. P.; Haste, N. M.; Taylor, S. S.; Eyck, L. F. Surface comparison of active and inactive protein kinases identifies a conserved activation mechanism. *Proc. Natl. Acad. Sci. U. S. A.* **2006**, *103* (47), 17783–17788.
- (52) Olivieri, C.; Li, G. C.; Wang, Y.; M, V. S.; Walker, C.; Kim, J.; Camilloni, C.; De Simone, A.; Vendruscolo, M.; Bernlohr, D. A. ATP-competitive inhibitors modulate the substrate binding cooperativity of a kinase by altering its conformational entropy. *Sci. Adv.* **2022**, *8* (30), No. eabo0696.
- (53) Becher, I.; Savitski, M. M.; Savitski, M. F.; Hopf, C.; Bantscheff, M.; Drewes, G. Affinity profiling of the cellular kinome for the nucleotide cofactors ATP, ADP, and GTP. *ACS Chem. Biol.* **2013**, *8* (3), 599–607.
- (54) Shamsi, Z.; Shukla, D. How does evolution design functional free energy landscapes of proteins? A case study on the emergence of regulation in the Cyclin Dependent Kinase family. *Molecular Systems Design & Engineering* **2020**, *5* (1), 392–400.
- (55) Masterson, L. R.; Shi, L.; Metcalfe, E.; Gao, J.; Taylor, S. S.; Veglia, G. Dynamically committed, uncommitted, and quenched states encoded in protein kinase A revealed by NMR spectroscopy. *Proc. Natl. Acad. Sci. U. S. A.* **2011**, *108* (17), 6969–6974.
- (56) Kim, J.; Ahuja, L. G.; Chao, F. A.; Xia, Y.; McClendon, C. L.; Kornev, A. P.; Taylor, S. S.; Veglia, G. A dynamic hydrophobic core orchestrates allostery in protein kinases. *Sci. Adv.* **2017**, *3* (4), No. e1600663.
- (57) Ahuja, L. G.; Taylor, S. S.; Kornev, A. P. Tuning the “violin” of protein kinases: The role of dynamics-based allostery. *IUBMB Life* **2019**, *71* (6), 685–696.
- (58) Shukla, D.; Meng, Y.; Roux, B.; Pande, V. S. Activation pathway of Src kinase reveals intermediate states as targets for drug design. *Nat. Commun.* **2014**, *5*, 3397.
- (59) Arora, M.; Moser, J.; Hoffman, T. E.; Watts, L. P.; Min, M.; Musteanu, M.; Rong, Y.; Ill, C. R.; Nangia, V.; Schneider, J. Rapid adaptation to CDK2 inhibition exposes intrinsic cell-cycle plasticity. *Cell* **2023**, *186* (12), 2628–2643.e2621.
- (60) Slabicki, M.; Kozicka, Z.; Petzold, G.; Li, Y. D.; Manojkumar, M.; Bunker, R. D.; Donovan, K. A.; Sievers, Q. L.; Koeppl, J.; Suchyta, D. The CDK inhibitor CR8 acts as a molecular glue degrader that depletes cyclin K. *Nature* **2020**, *585* (7824), 293. Zhang, J.; Gan, Y.; Li, H.; Yin, J.; He, X.; Lin, L.; Xu, S.; Fang, Z.; Kim, B. W.; Gao, L.; et al. Inhibition of the CDK2 and Cyclin A complex leads to autophagic degradation of CDK2 in cancer cells. *Nat. Commun.* **2022**, *13* (1), 2835.
- (61) Markwick, P. R.; Malliavin, T.; Nilges, M. Structural biology by NMR: structure, dynamics, and interactions. *Plos Comput. Biol.* **2008**, *4* (9), No. e1000168. Williamson, M. P. Using chemical shift perturbation to characterize ligand binding. *Prog. Nucl. Magn. Reson. Spectrosc.* **2013**, *73*, 1–16.
- (62) Masterson, L. R.; Mascioni, A.; Traaseth, N. J.; Taylor, S. S.; Veglia, G. Allosteric cooperativity in protein kinase A. *Proc. Natl. Acad. Sci. U. S. A.* **2008**, *105* (2), 506–511.
- (63) Kaoud, T. S.; Johnson, W. H.; Ebel, N. D.; Piserchio, A.; Zamora-Olivares, D.; Van Ravenstein, S. X.; Pridgen, J. R.; Edupuganti, R.; Sammons, R.; Cano, M.; et al. Modulating multi-functional ERK complexes by covalent targeting of a recruitment site in vivo. *Nat. Commun.* **2019**, *10* (1), 5232. Chu, N.; Viennet, T.; Bae, H.; Salguero, A.; Boeszoermyenyi, A.; Arthanari, H.; Cole, P. A. The structural determinants of PH domain-mediated regulation of Akt revealed by segmental labeling. *Elife* **2020**, *9*, 9. Kamski-Hennekam, E. R.; Huang, J.; Ahmed, R.; Melacini, G. Toward a molecular mechanism for the interaction of ATP with alpha-synuclein. *Chem. Sci.* **2023**, *14* (36), 9933–9942.
- (64) Majumdar, A.; Burban, D. J.; Muretta, J. M.; Thompson, A. R.; Engel, T. A.; Rasmussen, D. M.; Subrahmanian, M. V.; Veglia, G.; Thomas, D. D.; Levinson, N. M. Allostery governs Cdk2 activation and differential recognition of CDK inhibitors. *Nat. Chem. Biol.* **2021**, *17* (4), 456–464.
- (65) Nussinov, R.; Tsai, C. J.; Jang, H. Dynamic Protein Allosteric Regulation and Disease. *Adv. Exp. Med. Biol.* **2019**, *1163*, 25–43. Nussinov, R.; Tsai, C. J.; Ma, B. The underappreciated role of allostery in the cellular network. *Annual Review of Biophysics* **2013**, *42*, 169–189. Mathy, C. J. P.; Kortemme, T. Emerging maps of allosteric regulation in cellular networks. *Curr. Opin Struct. Biol.* **2023**, *80*, No. 102602. Martinez Pomier, K.; Akimoto, M.; Byun, J. A.; Khamina, M.; Melacini, G. Allosteric regulation of cyclic nucleotide-dependent protein kinases. *Can. J. Chem.* **2022**, *100* (9), 649–659.
- (66) Nussinov, R.; Zhang, M.; Maloney, R.; Liu, Y.; Tsai, C. J.; Jang, H. Allostery: Allosteric Cancer Drivers and Innovative Allosteric Drugs. *J. Mol. Biol.* **2022**, *434* (17), No. 167569.
- (67) Scheerer, D.; Adkar, B. V.; Bhattacharyya, S.; Levy, D.; Iljina, M.; Riven, I.; Dym, O.; Haran, G.; Shakhnovich, E. I. Allosteric communication between ligand binding domains modulates substrate inhibition in adenylate kinase. *Proc. Natl. Acad. Sci. U. S. A.* **2023**, *120* (18), No. e2219855120.
- (68) Arter, C.; Trask, L.; Ward, S.; Yeoh, S.; Bayliss, R. Structural features of the protein kinase domain and targeted binding by small-molecule inhibitors. *J. Biol. Chem.* **2022**, *298* (8), No. 102247.
- (69) McClendon, C. L.; Kornev, A. P.; Gilson, M. K.; Taylor, S. S. Dynamic architecture of a protein kinase. *Proc. Natl. Acad. Sci. U. S. A.* **2014**, *111* (43), E4623–E4631.
- (70) Fabbro, D.; Cowan-Jacob, S. W.; Moebitz, H. Ten things you should know about protein kinases: IUPHAR Review 14. *Br. J. Pharmacol.* **2015**, *172* (11), 2675–2700.
- (71) Meharena, H. S.; Fan, X.; Ahuja, L. G.; Keshwani, M. M.; McClendon, C. L.; Chen, A. M.; Adams, J. A.; Taylor, S. S. Decoding the Interactions Regulating the Active State Mechanics of Eukaryotic Protein Kinases. *PLoS Biol.* **2016**, *14* (11), No. e2000127.
- (72) Coleman, K. G.; Wautlet, B. S.; Morrissey, D.; Mulheron, J.; Sedman, S. A.; Brinkley, P.; Price, S.; Webster, K. R. Identification of CDK4 sequences involved in cyclin D1 and p16 binding. *J. Biol. Chem.* **1997**, *272* (30), 18869–18874.
- (73) Persky, N. S.; Hernandez, D.; Do Carmo, M.; Brenan, L.; Cohen, O.; Kitajima, S.; Nayar, U.; Walker, A.; Pantel, S.; Lee, Y.; et al. Defining the landscape of ATP-competitive inhibitor resistance residues in protein kinases. *Nat. Struct. Mol. Biol.* **2020**, *27* (1), 92–104.
- (74) Kim, D. M.; Yang, K.; Yang, B. S. Biochemical characterizations reveal different properties between CDK4/cyclin D1 and CDK2/cyclin A. *Exp. Mol. Med.* **2003**, *35* (5), 421–430.
- (75) Koivomagi, M.; Ord, M.; Iofik, A.; Valk, E.; Venta, R.; Faustova, I.; Kivi, R.; Balog, E. R.; Rubin, S. M.; Loog, M. Multisite phosphorylation networks as signal processors for Cdk1. *Nat. Struct. Mol. Biol.* **2013**, *20* (12), 1415–1424.

(76) Taylor, S. S.; Shaw, A. S.; Kannan, N.; Kornev, A. P. Integration of signaling in the kinase: Architecture and regulation of the alphaC Helix. *Biochim. Biophys. Acta* **2015**, *1854* (10 Pt B), 1567–1574. Shevchenko, E.; Pantsar, T. Regulatory spine RS3 residue of protein kinases: a lipophilic bystander or a decisive element in the small-molecule kinase inhibitor binding? *Biochem. Soc. Trans.* **2022**, *50* (1), 633–648. Mohanty, S.; Oruganty, K.; Kwon, A.; Byrne, D. P.; Ferries, S.; Ruan, Z.; Hanold, L. E.; Katiyar, S.; Kennedy, E. J.; Eyers, P. A.; Kannan, N. Hydrophobic Core Variations Provide a Structural Framework for Tyrosine Kinase Evolution and Functional Specialization. *Plos Genet* **2016**, *12* (2), No. e1005885.

(77) Azam, M.; Seeliger, M. A.; Gray, N. S.; Kuriyan, J.; Daley, G. Q. Activation of tyrosine kinases by mutation of the gatekeeper threonine. *Nat. Struct. Mol. Biol.* **2008**, *15* (10), 1109–1118.

(78) Hu, J.; Stites, E. C.; Yu, H.; Germino, E. A.; Meharena, H. S.; Stork, P. J. S.; Kornev, A. P.; Taylor, S. S.; Shaw, A. S. Allosteric activation of functionally asymmetric RAF kinase dimers. *Cell* **2013**, *154* (5), 1036–1046.

(79) Nussinov, R. Introduction to Protein Ensembles and Allostery. *Chem. Rev.* **2016**, *116* (11), 6263–6266.

(80) Kannan, N.; Haste, N.; Taylor, S. S.; Neuwald, A. F. The hallmark of AGC kinase functional divergence is its C-terminal tail, a cis-acting regulatory module. *Proc. Natl. Acad. Sci. U. S. A.* **2007**, *104* (4), 1272–1277. Reinhardt, R.; Leonard, T. A. A critical evaluation of protein kinase regulation by activation loop autophosphorylation. *Elife* **2023**, *12*, 12.

(81) Topacio, B. R.; Zatulovskiy, E.; Cristea, S.; Xie, S.; Tambo, C. S.; Rubin, S. M.; Sage, J.; Koivomagi, M.; Skotheim, J. M. Cyclin D-Cdk4,6 Drives Cell-Cycle Progression via the Retinoblastoma Protein's C-Terminal Helix. *Mol. Cell* **2019**, *74* (4), 758–770.e754.

(82) Maloney, R. C.; Zhang, M.; Jang, H.; Nussinov, R. The mechanism of activation of monomeric B-Raf V600E. *Comput. Struct. Biotechnol. J.* **2021**, *19*, 3349–3363. Zhang, M.; Maloney, R.; Liu, Y.; Jang, H.; Nussinov, R. Activation mechanisms of clinically distinct B-Raf V600E and V600K mutants. *Cancer Commun. (Lond)* **2023**, *43* (3), 405–408.

(83) Nussinov, R.; Zhang, M.; Maloney, R.; Tsai, C. J.; Yavuz, B. R.; Tuncbag, N.; Jang, H. Mechanism of activation and the rewired network: New drug design concepts. *Med. Res. Rev.* **2022**, *42* (2), 770–799. Zhang, M.; Jang, H.; Nussinov, R. PI3K inhibitors: review and new strategies. *Chem. Sci.* **2020**, *11* (23), 5855–5865.

(84) Faber, E. B.; Sun, L.; Tang, J.; Roberts, E.; Ganeshkumar, S.; Wang, N.; Rasmussen, D.; Majumdar, A.; Hirsch, L. E.; John, K.; et al. Development of allosteric and selective CDK2 inhibitors for contraception with negative cooperativity to cyclin binding. *Nat. Commun.* **2023**, *14* (1), 3213.

(85) Amaral, M.; Kokh, D. B.; Bomke, J.; Wegener, A.; Buchstaller, H. P.; Eggenweiler, H. M.; Matias, P.; Sirrenberg, C.; Wade, R. C.; Frech, M. Protein conformational flexibility modulates kinetics and thermodynamics of drug binding. *Nat. Commun.* **2017**, *8* (1), 2276.